HNF1alpha inactivation promotes lipogenesis in human hepatocellular adenoma independently of SREBP-1 and carbohydrate-response element-binding protein (ChREBP) activation.

Sandra Rebouissou, Sandrine Imbeaud, Charles Balabaud, Virginie Boulanger, Justine Bertrand-Michel, François Tercé, Charles Auffray, Paulette Bioulac-Sage, Jessica Zucman-Rossi

HNF1α INACTIVATION PROMOTES LIPOGENESIS IN HUMAN HEPATOCELLULAR ADENOMA INDEPENDENTLY OF SREBP-1 AND ChREBP ACTIVATION

Sandra Rebouissou[1,2], Sandrine Imbeaud[3], Charles Balabaud[4,5], Virginie Boulanger[3], Justine Bertrand-Michel[7], François Tercé[7], Charles Auffray[3], Paulette Bioulac-Sage[4,6], and Jessica Zucman-Rossi[1,2]

[1]Inserm, U674, Génomique fonctionnelle des tumeurs solides, Paris, France
[2]Université Paris 7 Denis Diderot, Institut Universitaire d'Hématologie, CEPH, Paris, France
[3]Array s/IMAGE, Genexpress, Functional Genomics and Systems Biology for Health - UMR 7091, CNRS, Université Paris 6 Pierre et Marie Curie, Villejuif, France
[4]Inserm, E362, Université Bordeaux 2, IFR66, Bordeaux, France
[5]CHU Bordeaux, Hôpital Saint-André, Bordeaux, France
[6]CHU Bordeaux, Hôpital Pellegrin, Bordeaux, France
[7] Lipidomic Platform, Inserm, IFR30, Génopole Toulouse, CHU Purpan, Toulouse, France

Running title: HNF1α inactivation promotes hepatic lipogenesis

Address correspondance to: Jessica Zucman-Rossi, Inserm, U674, Institut Universitaire d'Hématologie, CEPH, 27 rue Juliette Dodu, 75010 Paris, Tel. 33 1 53 72 51 66; FAX. 33 1 53 72 51 58; E-Mail: zucman@cephb.fr

Biallelic inactivating mutations of the transcription factor 1 gene (*TCF1*), encoding hepatocyte nuclear factor 1α (HNF1α), were identified in 50% of hepatocellular adenomas (HCA) phenotypically characterized by a striking steatosis. To understand the molecular basis of this aberrant lipid storage, we performed a microarray transcriptome analysis validated by quantitative RT-PCR, western-blotting and lipid profiling. In mutated HCA, we showed a repression of gluconeogenesis coordinated with an activation of glycolysis, citrate shuttle and fatty acid synthesis predicting elevated rates of lipogenesis. Moreover, the strong dowregulation of L-FABP suggests that impaired fatty acid trafficking may also contribute to the fatty phenotype. In addition, transcriptional profile analysis of the observed deregulated genes in non-HNF1α-mutated HCA as well as in non-tumor livers allowed us to define a specific signature of the HNF1α-mutated HCA. In theses tumors, lipid composition was dramatically modified according to the transcriptional deregulations identified in the fatty acid synthetic pathway. Surprisingly, lipogenesis activation did not operate through SREBP-1 and ChREBP that were repressed. We conclude that steatosis in HNF1α-mutated HCA results mainly from an aberrant promotion of lipogenesis that is linked to HNF1α inactivation and that is independent of both SREBP-1 and ChREBP activation. Finally, our findings have potential clinical implications since lipogenesis can be efficiently inhibited by targeted therapies.

Hepatocyte nuclear factor 1-α (HNF1α) is a transcription factor that controls the expression of liver-specific genes, such as β-fibrinogen, α1-antitrypsin and albumin (1). Heterozygous germline mutations in the gene encoding HNF1α (*TCF1*) are responsible for an autosomal dominant form of non-insulin-dependent diabetes mellitus called maturity onset diabetes of the young type 3 (MODY3), in which subjects usually develop hyperglycemia before 25 years of age (2). More recently, we identified HNF1α as a tumor suppressor gene involved in human liver tumorigenesis, since we found biallelic inactivating mutations of this gene in 50% of hepatocellular adenomas (HCA) and in rare cases of well-differentiated hepatocellular carcinomas developed in the absence of cirrhosis (3). HCA are rare benign primary liver tumors closely related to oral contraceptive intake (4).

Recently, in a comprehensive analysis of genotype-phenotype correlations in a large series of 96 HCA, we showed that HNF1α mutations define an homogeneous group of tumors phenotypically characterized by the recurrent presence of a marked steatosis (5). To get insight into the underlying molecular mechanisms that drive the fatty phenotype in human HNF1α-

mutated HCA, we performed a transcriptome analysis using cDNA and Affymetrix microarrays. Gene expression profiles were compared between non-tumor livers and HNF1α-mutated HCA. Among the differentially expressed genes we focused our analysis on genes involved in lipid homeostasis and we searched for a possible alteration in fat transport, degradation and synthesis processes. Transcriptomic deregulations were further validated in an additional series of tumors, but also at the protein level and we analyzed the precise composition of accumulated lipids.

EXPERIMENTAL PROCEDURES

Patients and samples. A series of 40 HCA, 25 non steatotic non-tumor livers and 11 steatotic non-tumor livers were collected in 9 French surgery departments from 1992 to 2004. Liver tissues were immediately frozen in liquid nitrogen and stored at -80°C until used for molecular studies. Among the 38 patients with an HCA, the sex ratio (M:F) was 1:9 and the mean age was 37 (median=37 years ranging from 14 to 56). All the patients were recruited in accordance with French law and institutional ethical guidelines. The study was approved by the ethical committee of Hôpital Saint-Louis, Paris, France. All HCA were screened for HNF1α and ß-catenin mutation, pathological slides were reviewed and all HCA were classified as previously described (5). Twenty five HCA from 23 patients were HNF1α-mutated, 11 demonstrated steatosis in more than 2/3 of hepatocytes, 8 in 1/3 to 2/3 of hepatocytes, 3 in less than 1/3 and 3 were not steatotic. Fifteen HCA had no mutations in HNF1α, four of them were β-catenin mutated, five were inflammatory and 9 demonstrated steatosis. Non-tumor liver tissues were taken from patients resected with primary liver tumors developed in the absence of cirrhosis. Steatotic non-tumor livers demonstrated lipid storage either in more than 2/3 of hepatocytes (four cases) or in 1/3 to 2/3 of hepatocytes (7 cases), and were of various etiologies: HCV (one case), dysmetabolic syndrome (6 cases), alcohol (three cases), and unknown etiology (one case).

Microarray analysis. Total RNA was extracted from frozen tissues using Qiagen RNeasy kits (Qiagen) according to the manufacturer's instructions. RNA integrity was assessed using RNA 6000 nano chips and the Agilent 2100 Bioanalyzer. RNA quality control was performed as previously described (6). Transcriptional profiling of HNF1α-mutated HCA and non-tumor liver tissues was performed using two different microarray approches. MIAME-compliant data (7) have been deposited in Gene Expression Omnibus (GEO) at NCBI (http://www.ncbi.nlm.nih.gov/geo/) and are accessible through GEO Series accession number GSExxxx and GSExxxx. Detailed procedure of analysis is provided in the supplemental experimental procedures.

Quantitative RT-PCR. Quantitative RT-PCR was performed as previously described (8) using pre-designed primers and probe sets from Applied Biosystems for the detection of *R18S*, *FABP1*, *PCK1*, *PCK2, FBP1*, *G6PT1*, *GCK*, *GCKR*, *GPI*, *ME1*, *MDH1*, *ACLY*, *PKLR*, *PKM2* (detection of both *PKM1* and *PKM2* transcripts), *ACACA*, *FASN*, *ELOVL1*, *ELOVL2*, *ELOVL5*, *SCD*, *FADS1, FADS2, SREBP-1* (detection of both *SREBP-1a* and *SREBP-1c* isoforms), *SREBP-1a, CHREBP, PPARα, PPARγ, LXRα* and *HNF4α.* Ribosomal 18S *(R18S)* was used for the normalization of expression data. The relative amount of measured mRNA in samples, was determined using the $2^{-\Delta\Delta CT}$ method where $\Delta\Delta CT = (CT_{target}\text{-}CT_{R18S})_{sample} - (CT_{target}\text{-}CT_{R18S})_{calibrator}$. Final results were expressed as the n-fold differences in target gene expression in tested samples compared to the mean expression value of non-tumor tissues.

Western blotting. Total protein extracts were obtained after homogenization in RIPA lysis buffer (Santa Cruz Biotechnology). Nuclear extracts were prepared using the NE-PER nuclear and cytoplasmic extraction reagent kit (Pierce) and protein concentration was determined using a Pierce BCA protein assay kit. Primary antibodies were used at the following dilutions: rabbit polyclonal anti-L-FABP 1:2000 (a gift of Dr. J Gordon), mouse monoclonals anti-FAS and anti-SREBP-1 (detecting both the SREBP-1a and SREBP-1c isoforms) 1:500 (BD Bioscience Pharmingen), polyclonals rabbit anti-GK (Santa Cruz Biotechnology) and anti-ACL (Cell Signaling Technology) 1:200, polyclonal rabbit anti-ChREBP 1:1000 (Novus Biologicals). We used polyclonal rabbit anti-actin (1:3000, Sigma) and polyclonal rabbit anti-Lamin A/C (1:500, Cell Signaling Technology) as loading controls to normalize the signal obtained respectively for total and nuclear protein

extracts. Detection of signals was performed using the ECL SuperSignal West Pico Chemiluminescent Substrate (Pierce) with either anti-mouse (1:4000, Amersham) or anti-rabbit (1:2000, Santa Cruz Biotechnology) horseradish peroxidase-conjugated IgG as second antibodies.

Glucose-6-phosphate measurement. Glucose-6-phosphate (G6P) concentrations were determined enzymatically in normal and tumor samples by exploiting the selective and quantitative conversion of G6P to 6-phosphogluconic acid in presence of $NADP^+$ and G6PDH, as previously described (9).

Histochemical analysis of glycogen storage. For this analysis, we used liver tissues frozen through immersion in isopentane cooled in liquid nitrogen. PAS histochemical staining was performed on frozen section from 5 HNF1α-mutated HCA and 5 non-mutated HCA as well as their matched non-tumor livers.

Lipid profiling. Detailed protocols used for lipid profiling are provided in the supplemental experimental procedures.

Statistical analysis. All the values reported are mean ± SD. Statistical analysis was performed using GraphPad Prism version 4 software and significance was determined using the nonparametric Mann-Whitney test for unpaired data. Difference was considered significant at $P<0.05$.

RESULTS

Gene expression profiles in HNF1α-mutated HCA. Our cDNA and Affymetrix microarray experiments analyzed the expression of a total of 15,000 different genes comparing respectively 8 HNF1α-mutated HCA to their corresponding non-tumor liver and five HNF1α-mutated HCA to four non-tumor livers. Computational analysis of both experiments identified 375 and 222 genes respectively significantly down and upregulated in HNF1α-mutated HCA. Among these genes, a large fraction was related to the normal hepatocyte function including carbohydrate and lipid metabolism, detoxification and synthesis of secreted proteins such as complement and coagulation factors (Supplemental Table 1). Among differentially expressed genes, promoter regions of 33 were previously identified to bound HNF1α in primary human hepatocytes using ChIP-on-chip technology (10). All but four of theses genes were downregulated in HNF1α-mutated HCA (Supplemental Table 1), which is in accordance with the well-known transactivating function of HNF1α. In addition, we identified 82 genes showing a common pattern of expression with liver from *hnf1α*-null mice (11) (Supplemental Table 1). Interestingly, 19 of these common deregulated genes were involved in glucido-lipidic metabolism and particularly in bile acid metabolism, cholesterol and fatty acid synthesis (Supplemental Table 1).

Fatty acid transport and oxidation. In HNF1α-mutated HCA, we identified an important modification in the expression profiles of apolipoprotein genes. Particularly, components of the HDL particles encoded by *APOM*, *LPAL2*, *APOF*, *LPA* and *APOA4* were strongly downregulated while *APOL3* was upregulated (Supplemental Table 1). In contrast, the expression of critical genes for hepatocyte VLDL assembly and secretion such as *APOB* and *MTP* was not affected. We also found a dramatic decrease in the mRNA of *FABP1* encoding the liver fatty acid binding protein (L-FABP). This result was confirmed by quantitative RT-PCR (-68-fold change, Figure 1A) and by western-blotting analysis that showed an absence of L-FABP in mutated HCA (Figure 1B). In contrast, we did not find any change in the expression of genes encoding mitochondrial and peroxisomal β-oxidation enzymes. The expression level of genes encoding plasma membrane transporters such as *CD36* was also normal in mutated HCA as well as the LDL receptor gene. However, we identified a number of deregulated genes related to the lipogenesis pathway (Figures 2A and 3A).

Gluconeogenesis repression and glycolysis activation. The expression of four genes (*FBP1* encoding the fructose-1,6-bisphosphatase, *PCK1* and *PCK2* encoding respectively the cytosolic and the mitochondrial forms of the PEPCK enzyme and *G6PT1* encoding the glucose-6-phosphate transporter 1) critical to promote hepatic glucose production was significantly decreased in HNF1α-mutated HCA (Figure 2B), indicating a repression of the gluconeogenesis pathway in these tumors (Figure 2A). In contrast, glycolysis was activated in HNF1α-mutated HCA, since we found a strong upregulation of

glucokinase at the mRNA (*GCK*, 11-fold) and protein level (GK, Figure 2B and 2C). In addition, we found a 3-fold decrease in the expression of the *GCKR* transcript whose product acts as a negative regulator of glucokinase (Figure 2B). According to a predicted increased glucose phosphorylation rate, we showed a significantly higher level of glucose-6-phosphate in HNF1α-mutated HCA (Figure 2D). Moreover, PAS staining revealed a glycogen overload in these tumors consistent with G6P increase (Figure 2E). We also found an upregulation of *GPI* mRNA (4-fold, Figure 2B) which encodes the glucose phosphate isomerase, a second glycolytic enzyme. In contrast, *PKLR* mRNA which encodes the liver specific pyruvate kinase that catalyzes the last irreversible step of glycolysis was 3-fold decreased in HNF1α-mutated HCA (Figure 2F). However, *PKLR* downregulation may be balanced by a 2-fold increase of *PKM2* gene that encodes the muscle specific pyruvate kinase (Figure 2F).

Activation of the citrate shuttle. Besides the observed gluconeogenesis inhibition and glycolysis activation that predict an overproduction of pyruvate, a substrate for the mitochondrial synthesis of acetylCoA, the citrate shuttle system that export acetylCoA into the cytosol was also activated in HNF1α-mutated HCA (Figure 2A). Indeed, we found a 12-fold overexpression of *ME1* mRNA which encodes the malic enzyme, a moderate 2-fold increase of *MDH1* transcript and *ACLY* mRNA encoding the ATP citrate lyase (ACL) was 3.7-fold overexpressed in HNF1α-mutated HCA (Figure 2B). As ATP citrate lyase is crucial to provide the unique cytoplasmic source of the acetylCoA lipogenic precursor, we confirmed by western-blotting the ACL protein overexpression (Figure 2C).

Stimulation of the fatty acid synthetic pathway. As shown in Figure 3A, the fatty acid synthetic pathway was also stimulated in HNF1α-mutated HCA. We found an increase of the acetyl-CoA carboxylase transcript (*ACACA*, 2.6-fold) and a strong overexpression of fatty acid synthase at both trancriptional (*FASN*, 7-fold) and protein level (FAS, Figures 3B and 3C). In the downstream steps of fatty acid elongation and desaturation, we also identified an increase in the mRNA level of three genes encoding elongases including *ELOVL1* (3.4-fold), *ELOVL2* (2.2-fold) and *ELOVL5* (2.3-fold) and of three genes encoding desaturases such as *SCD* (6-fold), *FADS1* (3-fold) and *FADS2* (4.7-fold, Figure 3B).

Transcriptional alteration of glucido-lipidic genes defines an expression pattern that is specific of HNF1α-mutated HCA. To search if the pattern of alteration in the expression of the glucido-lipidic genes was specific of HNF1α inactivation, we compared the expression profiles of the 19 aforementioned genes between HNF1α-mutated HCA and a group of non-mutated HCA containing or not steatosis, using quantitative RT-PCR. In this analysis, we also included steatotic non-tumor livers from different etiologies and non steatotic non-tumor livers. We then performed a non-supervised analysis of the results using a hierarchical clustering algorithm to group the genes as well as the samples on the basis of similarity in their expression pattern. This analysis accurately classified all samples in two major clusters according to their HNF1α status (Figure 4). Steatotic non-tumor livers and non-steatotic non-tumor livers were gathered with the non-HNF1α-mutated HCA. Gene cluster analysis identified two main groups corresponding to downregulated (cluster A) and upregulated (cluster B) genes in HNF1α-mutated HCA (Figure 4). As expected, four out of five genes identified in cluster A had been previously characterized as HNF1α transactivated targets. Interestingly, all upregulated genes have never been previously found regulated by HNF1α. Within cluster B, three subgroups of genes (1, 2, 3) showed a highly correlated overexpression in HNF1α-mutated HCA (Supplemental Figure 1). For example, *ACLY* level of expression was correlated to *ACACA* overexpression in 16 HNF1α-mutated HCA (Spearman r=0.72, *P*=0.001) (Supplemental Figure 1).

In non-HNF1α-mutated liver tissues, only few genes demonstrated a significant transcriptional deregulation (Supplemental Figure 2). In steatotic non-tumor livers, expression of only two genes, *PCK2* and *ME1,* followed an expression pattern as seen in HNF1α-mutated HCA (Supplemental Figure 2). In non-HNF1α-mutated steatotic HCA, 9 genes involved in gluconeogenesis, glycolysis and citrate shuttle were significantly deregulated compared to the non-steatotic non-tumor livers (Supplemental Figure 2). One of these, *GCK*, showed an inversed pattern of deregulation when compared

to the HNF1α-mutated HCA. However, except a modest elevation in *ELOVL1* transcript, expression of genes related to the fatty acid synthetic pathway were unchanged in this group of steatotic adenomas. Finally, in the group of non-HNF1α-mutated non-steatotic HCA only four genes showed a significant change in expression pattern (*FBP1*, *GPI*, *ACLY*, *ELOVL1*).

These results indicated that patterns of expression of the 19 analyzed genes were specific to HNF1α inactivation. Downregulations could be directly attributed to the loss of the classical HNF1α transactivation activity. In contrast, overexpressed genes demonstrated a coordinated activation, but none are known to date to be directly controlled by HNF1α.

Activation of lipogenesis in HNF1α-mutated HCA is independent of SREBP-1 and ChREBP activation. Among the lipogenic genes whose expression was increased in HNF1α-mutated HCA, 8 out of 13 were previously described as SREBP-1c targets. However, using quantitative RT-PCR, we did not find any significant variation in the mRNA level of total *SREBP-1* in HNF1α-mutated HCA compared to non-tumor livers, nor in *SREBP-1a* (Figure 6A). Moreover, surprisingly, western-blotting studies revealed a decrease in the nuclear active form of SREBP-1 in the tumors compared to their corresponding non-tumor liver (Figure 6B), and the microarray study also found an increase in *INSIG1* (insulin induced gene 1) mRNA (2 fold, Supplemental Table 1) whose product is known to inhibit SREBP-1 cleavage processing. We then looked for a potential alteration of ChREBP expression, an other key transcriptional activator of fatty acid synthesis in the liver. RT-PCR results showed a significant decrease in the mRNA of *CHREBP* in HNF1α-mutated HCA (-1.8-fold, Figure 6A) and western blotting studies revealed a decrease of the protein level in the nucleus (Figure 6B). Using the same samples where we demonstrated a repression of both SREBP-1 and ChREBP, we found an obvious overexpression of the fatty acid synthase (FAS) and glucokinase (GK) proteins, which are known to be transactivated by these two transcription factors (Figure 6B). Although unexpected, these results suggest that increased lipogenic genes expression found in HNF1α-mutated HCA is not related to SREBP-1 and ChREBP activation. FAS and GK overexpression were confirmed in three additional cases of HNF1α-mutated HCA (Supplemental Figure 3). In two of these three cases, ChREBP was decreased and the nuclear active form of SREBP-1 was highly reduced or unchanged. In the remaining case we found a mild elevation of ChREBP and nuclear SREBP-1 compared to the non-tumoral counterpart. On the whole, we observed an increased expression of FAS and GK together with a clear repression of SREBP-1 and ChREBP in four out of 6 HNF1α-mutated HCA analyzed. Interestingly, no similar pattern of expression was found in the non-HNF1α-mutated HCA tested (Supplemental Figure 3). We also checked for the transcriptional level of other transcription factors that have been implicated in the regulation of glucido-lipidic metabolism (Figure 6A). Except for a 1.9-fold elevation of *PPARγ* transcript, the mRNA level of *FOXO1A, PPARα, LXRα* and *HNF4α* was not significantly different in HNF1α-mutated HCA compared to non-tumor livers (Figure 6A). Finally, the *RXR* isotypes genes were not differentially expressed in the microarray analysis.

Total lipid composition is modified in HNF1α-mutated HCA. We compared lipid profiles of four non-steatotic non-tumor livers with that of five HNF1α-mutated HCA. Total fatty acid content was 5.8-fold increased in HNF1α-mutated HCA and the fatty acid profile was modified. Saturated (SFA) and monounsaturated (MUFA) fatty acids were 7- and 8-fold increased respectively, as a consequence of the accumulation of all SFA and MUFA species detected (Figure 3A, 5C and 5D). In contrast, polyunsaturated fatty acids (PUFA) were raised only 2-fold (Figure 5A) with a preferential accumulation of fatty acids containing 18 carbon atoms including the two essential fatty acids linoleic acid (18:2n-6) and α-linolenic acid (18:3n-3). Consequently, the SFA/PUFA and MUFA/PUFA ratios in mutated HCA were significantly higher than in non-tumor livers (Figure 5B). We also showed that C14-C18 fatty acids were much more increased than C20-C23 fatty acids, as indicated by a 5-fold higher C14-C18/C20-C23 ratio (Figure 5B). We also identified a mild elevation in free cholesterol content in HNF1α-mutated HCA (36 *vs* 26.2 nmol/mg of proteins, Figure 5F), however, we did not find any change neither in total cholesterol esters and diglycerides contents

(Figure 5F) nor in specific molecular species related to these two neutral lipid classes (data not shown). In contrast, total and all species of triglycerides were dramatically increased in HNF1α-mutated HCA (Figures 5F and 5G). This overload was inversely proportional to the total number of carbon atoms of each species (ranging from a 53-fold for C49 to a 4.8-fold increase for C57 families, Figure 5G), according to the highest increase in C14-C16 fatty acid species *versus* C18-C20.

Phospholipid profile is also changed in HNF1α-mutated HCA. As shown in Table 1, HNF1α-mutated HCA showed a 2-fold increase in total phospholipid quantity that was related to a significant elevation of phosphatidylcholine (PC) and phosphatidylethanolamine (PE), while content of the other phospholipid classes including sphingomyelin (SM) was unchanged compared to non-tumor livers (except for PS that was undetectable in the tumors). Our results also showed a significant elevation in the PE fraction whereas the PI fraction was reduced (Table 1), indicating that phospholipid profile was qualitatively changed. The fatty acid profile of PE was not significantly modified, while it was moderately alterated for PC and PS-PI classes (Table 2). In PS-PI, we found a significant elevation of the MUFA fraction (Table 2). In PC, the SFA and PUFA fractions were respectively decreased and increased, consequently, the PC-unsaturation index was significantly increased in HNF1α-mutated HCA (Table 2). We also showed that C20-C24 were over-represented in the PC fraction of HNF1α-mutated HCA, as indicated by the significant decrease of the C16-C18/C20-C24 ratio (1.8 fold). When analyzing fatty acid composition of the total phospholipids, we only found a reduction in the C16-C18/C20-C24 ratio in HNF1α-mutated HCA (Table 2).

DISCUSSION

In the present work, careful analysis of the metabolic pathways alterated in the HNF1α-mutated HCA may explain the severe fatty overload observed in these tumors. First, we identified a repression of gluconeogenesis coordinated with an activation of glycolysis and citrate shuttle predicting an aberrant accumulation of the acetylCoA and NADPH lipogenic precursors (12). In addition, these tumors also showed an obvious stimulation of the fatty acid synthetic pathway from palmitate synthesis to the downstream steps of fatty acid elongation and desaturation. Taken together, these findings provide evidence that *de novo* lipogenesis activity is increased in HNF1α-mutated HCA, and we showed that it is specifically related to the loss of HNF1α activity. The fact that the steatotic non-HNF1α-mutated HCA and the steatotic non-tumor livers did not show the same deregulated expression pattern as in mutated HCA suggests that lipid storage in these two groups of samples likely occurs independently of HNF1α inactivation. Moreover, since lipogenesis activity is known to be mainly regulated at the transcriptional level, it is unlikely that higher lipogenic rates would be a significant driver of fat accumulation in the steatotic non-HNF1α-mutated HCA or in the steatotic non-tumor livers. Indeed, in these two sample groups, no major transcriptional deregulation was found in the lipogenic pathway. However, it does not exclude a possible activation of lipogenesis at a post-transcriptional level. The importance of lipogenesis in human steatosis is still under discussion. Here, we report a particular situation in humans, in which hepatocyte steatosis developed in the context of HNF1α inactivation seems to be primarily due to an aberrant stimulation of lipogenic rate.

In mice, loss of HNF1α activity was also associated with the development of fatty liver (13,14), and a prior work identified a significant elevation in the liver expression of the acetyl-CoA carboxylase and fatty acid synthase genes (14). However, our study is the first one to demonstrate a coordinate overexpression of all lipogenic genes and to highlight the major involvement of this aberrant induction in the pathogenesis of fatty liver phenotype related to HNF1α inactivation. In the present work, we identified transcriptional deregulations of 19 genes that may explain fat overload observed in the human HNF1α-mutated HCA. Interestingly, when extracting the expression data from the transciptome analysis performed by Shih *et al.* in the liver from *hnf1α*-null mice, we found that 9 of theses 19 genes were commonly deregulated in mice. Moreover, it is remarkable that the most important overlap was found for the genes involved in the fatty acid synthetic pathway (5/9).

Among the 19 deregulated genes, three of the 6 downregulated genes (*FABP1*, *G6PT1* and *PCK1*) were previously demonstrated to be directly transactivated by HNF1α and promoter

region of *GCKR* has been shown to bind HNF1α *in vivo* by ChIP (10,14-16). However, among the overexpressed genes, the majority were known to be transactivated by the membrane bound transcription factor SREBP-1c. SREBP-1c is considered as the master regulator of fatty acid synthesis in the liver, mediating effects of insulin on the expression of glycolytic and lipogenic genes after being activated by proteolytic cleavage (17). Surprisingly, in HNF1α-mutated HCA, SREBP-1 was repressed in most of the cases, possibly resulting from the induction of *INSIG1* mRNA (18). This finding contrasts with that found in *hnf1α*-null mice liver in which a significant increase of *SREBP-1* transcript was reported (11). ChREBP is an other transcription factor known to activate the expression of some lipogenic genes such as *ACLY*, *ACACA*, *FASN* (19). In HNF1α-mutated HCA we also found a reduction of the ChREBP mRNA level and nuclear protein amounts, demonstrating repression. This could occur as a consequence of the observed PUFA elevation in the tumors and particularly of the linoleic acid, that has been shown to suppress ChREBP activity by increasing its mRNA decay and altering its translocation from the cytosol to the nucleus (20). Thus, the repression of SREBP-1 and ChREBP observed in most of the analyzed HNF1α-mutated HCA could result from a negative feedback responding to lipid overload. Furthermore, although a large fraction of SREBP-1 targets were overexpressed in HNF1α-mutated HCA, some well-known targets such as the 6-phosphogluconate dehydrogenase (6PGDH) and glucose-6-phosphate dehydrogenase (G6PDH), were not deregulated in mutated HCA. Altogether, our results imply that SREBP-1 and ChREBP are not responsible for the coordinate induction of glycolytic and lipogenic genes observed in HNF1α-mutated HCA. PPARγ was previously proposed to play a role in hepatic induction of lipogenic genes through a mechanism that is still unclear (21-23). In the HNF1α-mutated HCA, we found an increase in *PPARγ* gene expression, however, among three well-known targets of this transcription factor (*FABP4*, *CD36* and *UCP2)* only one demonstrated a significant overexpression (*FABP4* gene 5-fold, Supplemental Table 1) suggesting that PPARγ activity is not obviously increased in HNF1α-mutated HCA. Thus, the mechanism by which HNF1α inactivation leads to the coordinate overexpression of the lipogenic genes remains to be elucidated. The strong correlation groups identified between overexpressed transcripts suggest that a transcriptional mechanism would be most likely at the origin of the observed deregulations, instead of a post-transcriptional regulation such as mRNA stability. Consequently, transcriptional activation of the lipogenic genes related to HNF1α inactivation may occur through the loss of a direct HNF1α repressor function involving either direct DNA binding or interaction with others transcription factors and co-activator proteins (Supplemental Figure 4A). Although, HNF1α has been mainly reported as a transcriptional activator, this model would explain some of the identified overexpressions. Indeed a co-repressor activity for HNF1α on its own transcription has already been shown through interaction with HNF4α (24). Alternatively, the absence of a functional HNF1α protein may also alter the expression of another transcription factor involved in the control of lipogenesis (Supplemental Figure 4B). New insights into understanding the mechanisms regulating lipogenic gene expression by HNF1α could come from the analysis of gene promoter activity in cellular systems in which HNF1α activity will be modulated.

Results from lipid profiling analysis of the accumulated fat in HNF1α-mutated HCA are well correlated with the transcriptional deregulations observed in the fatty acid synthetic pathway. Indeed, the preferential accumulation of SFA and MUFA species is in accordance with the strong overexpression of *FAS* and *SCD*, and with the high elevation of *ELOVL1* expression (25-27). The significant accumulation of the two essential fatty acids linoleic acid and α-linolenic acid suggests that in addition to the elevated rates of lipogenesis, other mechanisms may contribute to the fatty phenotype in HNF1α-mutated HCA. This is unlikely the consequence of impaired VLDL secretion or fatty acid entry into the tumor hepatocytes, since no obvious deregulations in the expression of the genes involved in these processes was identified. However, although expression of fatty acid oxidation genes was unchanged in HNF1α-mutated HCA, it is likely that fatty acid oxidation is reduced in adenoma cells secondary to lipogenic rate increase. Indeed, this may occur through the inhibition of CPT1 activity resulting from the overproduction of malonyl-CoA by the

acetylCoA carboxylase whose transcript was significantly upregulated in HNF1α-mutated HCA. Thus, a secondary defect in β-oxidation may contribute to fat accumulation and may explain in part the observed elevation of essential fatty acids. Moreover, given the role of L-FABP in binding, trafficking and compartmentalization of fatty acids into the hepatocyte, the dramatic decrease in L-FABP expression may also participate to the steatotic phenotype, as suggested in *hnf1α*-null mice liver (28). The alteration of phospholipid profile in HNF1α-mutated HCA was moderate. However, it may cause deregulation of membrane functioning in adenoma cells leading to alteration of critical cellular processes related to tumorigenesis.

In this study, we clearly demonstrated that lipogenesis activity was increased in HNF1α-mutated HCA and this feature has been commonly observed in tumor cells. Indeed, overexpression of the fatty acid synthase was previously identified in a wide variety of cancers as well as in precancerous lesions (29). This overexpression was often accompanied by a coordinate induction of the other lipogenic enzymes and several studies have shown that tumor cell survival may depend on *de novo* synthesis of fatty acids. While the fatty acid synthase as been proposed as an interesting therapeutic target for cancer treatment, more recent studies showed that the inhibition of other lipogenic enzymes like acetylCoA carboxylase or ATP citrate lyase can also limit cancer cell proliferation and survival (30,31). Recently, we proposed HNF1α as a tumor suppressor gene (3) and we demonstrated in the present work, that lipogenesis activation in HNF1α-mutated HCA results from the loss of HNF1α activity. This finding may contribute to reinforce the emerging concept that induction of lipogenesis observed in tumor cells would occur downstream from oncogenic events (29) and open new avenues to understand how metabolism deregulations may contribute to benign liver tumorigenesis. Finally, our findings have potential clinical implications since lipogenesis can be efficiently inhibited by targeted therapies.

ACKNOWLEDGEMENTS

We warmly thank all the other participants to the GENTHEP (Groupe d'étude Génétique des Tumeurs Hépatiques) network. We are grateful to Emmanuelle Jeannot and Lucille Mellottee for their help in mutation screening and excellent technical assistance and Véronique Roques for helpful assistance at the Lipidomic Platform. We thank Dr J. Gordon for providing us the L-FABP antibody and Dr. RHJ Bandsma for the experimental procedure of glucose-6-phosphate measurement. We also thank Alain Paris and Philippe Bois for critical reading of the manuscript. This work was supported by the Inserm (Réseau de Recherche clinique et en santé des populations), ARC n°5188, SNFGE and the Fondation de France. SR is supported by a Ligue Nationale Contre le Cancer doctoral fellowship.

REFERENCES

1. Courtois, G., Morgan, J. G., Campbell, L. A., Fourel, G., and Crabtree, G. R. (1987) *Science* **238**(4827), 688-692
2. Yamagata, K., Oda, N., Kaisaki, P. J., Menzel, S., Furuta, H., Vaxillaire, M., Southam, L., Cox, R. D., Lathrop, G. M., Boriraj, V. V., Chen, X., Cox, N. J., Oda, Y., Yano, H., Le Beau, M. M., Yamada, S., Nishigori, H., Takeda, J., Fajans, S. S., Hattersley, A. T., Iwasaki, N., Hansen, T., Pedersen, O., Polonsky, K. S., Bell, G. I., and et al. (1996) *Nature* **384**(6608), 455-458
3. Bluteau, O., Jeannot, E., Bioulac-Sage, P., Marques, J. M., Blanc, J. F., Bui, H., Beaudoin, J. C., Franco, D., Balabaud, C., Laurent-Puig, P., and Zucman-Rossi, J. (2002) *Nat Genet* **32**(2), 312-315
4. Edmondson, H. A., Henderson, B., and Benton, B. (1976) *N Engl J Med* **294**(9), 470-472
5. Zucman-Rossi, J., Jeannot, E., Nhieu, J. T., Scoazec, J. Y., Guettier, C., Rebouissou, S., Bacq, Y., Leteurtre, E., Paradis, V., Michalak, S., Wendum, D., Chiche, L., Fabre, M., Mellottee, L., Laurent, C., Partensky, C., Castaing, D., Zafrani, E. S., Laurent-Puig, P., Balabaud, C., and Bioulac-Sage, P. (2006) *Hepatology* **43**(3), 515-524

6. Imbeaud, S., Graudens, E., Boulanger, V., Barlet, X., Zaborski, P., Eveno, E., Mueller, O., Schroeder, A., and Auffray, C. (2005) *Nucleic Acids Res* **33**(6), e56
7. Brazma, A., Hingamp, P., Quackenbush, J., Sherlock, G., Spellman, P., Stoeckert, C., Aach, J., Ansorge, W., Ball, C. A., Causton, H. C., Gaasterland, T., Glenisson, P., Holstege, F. C., Kim, I. F., Markowitz, V., Matese, J. C., Parkinson, H., Robinson, A., Sarkans, U., Schulze-Kremer, S., Stewart, J., Taylor, R., Vilo, J., and Vingron, M. (2001) *Nat Genet* **29**(4), 365-371
8. Rebouissou, S., Vasiliu, V., Thomas, C., Bellanne-Chantelot, C., Bui, H., Chretien, Y., Timsit, J., Rosty, C., Laurent-Puig, P., Chauveau, D., and Zucman-Rossi, J. (2005) *Hum Mol Genet* **14**(5), 603-614
9. Bandsma, R. H., Wiegman, C. H., Herling, A. W., Burger, H. J., ter Harmsel, A., Meijer, A. J., Romijn, J. A., Reijngoud, D. J., and Kuipers, F. (2001) *Diabetes* **50**(11), 2591-2597
10. Odom, D. T., Zizlsperger, N., Gordon, D. B., Bell, G. W., Rinaldi, N. J., Murray, H. L., Volkert, T. L., Schreiber, J., Rolfe, P. A., Gifford, D. K., Fraenkel, E., Bell, G. I., and Young, R. A. (2004) *Science* **303**(5662), 1378-1381
11. Shih, D. Q., Bussen, M., Sehayek, E., Ananthanarayanan, M., Shneider, B. L., Suchy, F. J., Shefer, S., Bollileni, J. S., Gonzalez, F. J., Breslow, J. L., and Stoffel, M. (2001) *Nat Genet* **27**(4), 375-382
12. Foufelle, F., and Ferre, P. (2002) *Biochem J* **366**(Pt 2), 377-391
13. Lee, Y. H., Sauer, B., and Gonzalez, F. J. (1998) *Mol Cell Biol* **18**(5), 3059-3068
14. Akiyama, T. E., Ward, J. M., and Gonzalez, F. J. (2000) *J Biol Chem* **275**(35), 27117-27122
15. Hiraiwa, H., Pan, C. J., Lin, B., Akiyama, T. E., Gonzalez, F. J., and Chou, J. Y. (2001) *J Biol Chem* **276**(11), 7963-7967
16. Yanuka-Kashles, O., Cohen, H., Trus, M., Aran, A., Benvenisty, N., and Reshef, L. (1994) *Mol Cell Biol* **14**(11), 7124-7133
17. Horton, J. D., Goldstein, J. L., and Brown, M. S. (2002) *J Clin Invest* **109**(9), 1125-1131
18. Engelking, L. J., Kuriyama, H., Hammer, R. E., Horton, J. D., Brown, M. S., Goldstein, J. L., and Liang, G. (2004) *J Clin Invest* **113**(8), 1168-1175
19. Iizuka, K., Bruick, R. K., Liang, G., Horton, J. D., and Uyeda, K. (2004) *Proc Natl Acad Sci U S A* **101**(19), 7281-7286
20. Dentin, R., Benhamed, F., Pegorier, J. P., Foufelle, F., Viollet, B., Vaulont, S., Girard, J., and Postic, C. (2005) *J Clin Invest* **115**(10), 2843-2854
21. Matsusue, K., Haluzik, M., Lambert, G., Yim, S. H., Gavrilova, O., Ward, J. M., Brewer, B., Jr., Reitman, M. L., and Gonzalez, F. J. (2003) *J Clin Invest* **111**(5), 737-747
22. Schadinger, S. E., Bucher, N. L., Schreiber, B. M., and Farmer, S. R. (2005) *Am J Physiol Endocrinol Metab* **288**(6), E1195-1205
23. Zhang, Y. L., Hernandez-Ono, A., Siri, P., Weisberg, S., Conlon, D., Graham Mark, J., Crooke, R. M., Huang, L. S., and Ginsberg, H. N. (2006) *J Biol Chem*
24. Ktistaki, E., and Talianidis, I. (1997) *Science* **277**(5322), 109-112
25. Smith, S. (1994) *Faseb J* **8**(15), 1248-1259
26. Ntambi, J. M., and Miyazaki, M. (2004) *Prog Lipid Res* **43**(2), 91-104
27. Jakobsson, A., Westerberg, R., and Jacobsson, A. (2006) *Prog Lipid Res* **45**(3), 237-249
28. Gordon, J. I., Elshourbagy, N., Lowe, J. B., Liao, W. S., Alpers, D. H., and Taylor, J. M. (1985) *J Biol Chem* **260**(4), 1995-1998
29. Swinnen, J. V., Brusselmans, K., and Verhoeven, G. (2006) *Curr Opin Clin Nutr Metab Care* **9**(4), 358-365
30. Hatzivassiliou, G., Zhao, F., Bauer, D. E., Andreadis, C., Shaw, A. N., Dhanak, D., Hingorani, S. R., Tuveson, D. A., and Thompson, C. B. (2005) *Cancer Cell* **8**(4), 311-321
31. Brusselmans, K., De Schrijver, E., Verhoeven, G., and Swinnen, J. V. (2005) *Cancer Res* **65**(15), 6719-6725

ABBREVIATIONS

ACACA, acetyl-CoA carboxylase-alpha; ACLY/ACL, ATP citrate lyase; CE, cholesterol esters; ChIP, chromatin immunoprecipitation; ChREBP, carbohydrate response element binding protein; DG, diglycerides; ELOVL1, elongation of very long chain fatty acids protein 1; ELOVL2, elongation of

very long chain fatty acids protein 2; ELOVL5, ELOVL family member 5, elongation of very long chain fatty acids; FA, fatty acids; FABP1/L-FABP, liver fatty acid binding protein; FADS1, fatty acid desaturase 1; FADS2, fatty acid desaturase 2; FASN/FAS, fatty acid synthase; FBP1, fructose-1,6-bisphosphatase; FOXO1A, forkhead box O1A; GCK/GK, glucokinase; GCKR, glucokinase regulatory protein; G6P, glucose-6-phosphate; GPI, glucose-6-phosphate isomerase; G6PT1, glucose-6-phosphate transporter 1; HCA, hepatocellular adenoma; HNF1α, hepatocyte nuclear factor 1-α; HNF4α, hepatocyte nuclear factor 4- alpha; INSIG1, insulin induced gene 1; LXRα, liver X receptor, alpha; ME1, malic enzyme 1; MODY3, maturity onset diabetes of the young type 3; MDH1, NADPH malate dehydrogenase, soluble; MUFA, monounsaturated fatty acids; PC, phosphatidylcholine; PCK1, phosphenolpyruvate carboxykinase 1, soluble; PCK2, phosphenolpyruvate carboxykinase 2, mithochondrial; PE, phosphatidylethanolamine; PKLR, pyruvate kinase, liver and red blood cell; PKM2, pyruvate kinase muscle 2; PL, phospholipids; PPARα, peroxisome proliferator-activated receptor-alpha; PPARγ, peroxisome proliferator-activated receptor-gamma; PS-PI, phosphatidylserine-phosphatidylinositol; PUFA, polyunsaturated fatty acids; SCD, stearoyl-CoA desaturase; SFA, saturated fatty acids; SM, sphingomyelin; SREBP-1, sterol regulatory element-binding protein-1; TCF1, transcription factor 1; TG, triglycerides; UFA, unsaturated fatty acids; UI, unsaturation index

FIGURES LEGENDS

Fig. 1. Expression of *FABP1* transcript and L-FABP protein in HNF1α-mutated HCA. A. mRNA level of *FABP1* gene was assessed using quantitative RT-PCR. Results are expressed as the n-fold difference in gene expression relative to the mean expression value of non-tumor livers. Data are mean ± SD. *** difference between groups at $P<0.001$**. B.** Protein level of L-FABP (14 kDa) was compared between 3 HNF1α-mutated HCA (T_1, T_2, T_3) and their respective corresponding non-tumor liver (N_1, N_2, N_3) using western-blotting. β-actin was used as loading control.

Fig. 2. Gluconeogenesis repression, glycolysis and citrate shuttle activation in HNF1α-mutated HCA. A. Schematic representation of gluconeogenic pathway (gray arrows), glycolytic pathway and citrate shuttle (black arrows). Dashed arrows indicate several reaction steps. Genes whose expression was deregulated in HNF1α-mutated HCA are in solid boxes. (↑) and (↓) indicate transcripts that are respectively upregulated and downregulated compared to non-tumor livers. * indicates a significant increase in the product quantity. **B.** Quantitative RT-PCR validation of gene array expression data. Results are expressed as the n-fold difference in gene expression relative to the mean expression value of non-tumor livers. Data are mean ± SD. *, **, *** difference between groups at $P<0.05$; 0.01 and 0.001 respectively. **C**. Protein level of GK (52 kDa) and ACL (125 kDa) was compared by western-blotting analysis between 2 HNF1α-mutated HCA (T_1, T_2) and their respective corresponding non-tumor liver (N_1, N_2). β-actin was used as loading control. **D**. G6P content measurement. Values are mean ± SD. ** difference between groups at $P<0.01$. **E**. Frozen sections of a non-HNF1α-mutated HCA (a) and an HNF1α-mutated HCA (b). Glycogen storage in cytoplasm of hepatocytes (red color with PAS staining) is increased in HNF1α-mutated HCA (b) compared with non-mutated HCA (a). **F**. mRNA level of *PKLR* and *PKM2* genes was assessed using quantitative RT-PCR. Results are expressed as the n-fold difference in gene expression relative to the mean expression value of non-tumor livers. Data are mean ± SD. *** difference between groups at $P<0.001$

Fig. 3. Activation of the fatty acid synthetic pathway in HNF1α-mutated HCA. A. Schematic representation of the fatty acid synthetic pathway. Dashed arrows indicate several reaction steps that occur only in plants. Genes whose expression was deregulated in HNF1α-mutated HCA are in solid boxes. (↑) indicates transcript upregulation compared to non-tumor livers. * indicates fatty acid species significantly raised in HNF1α-mutated HCA compared to non-tumor livers, FA: fatty acids. **B.** Quantitative RT-PCR validation of gene array expression data. Results are expressed as the n-fold difference in gene expression relative to the mean expression value of non-tumor livers. Data are mean ± SD. **, ***, difference between groups at $P<0.01$ and 0.001 respectively. **C**. Protein level

of FAS (265 kDa) was compared by western-blotting analysis between 2 HNF1α-mutated HCA (T_1, T_2) and their respective corresponding non-tumor liver (N_1, N_2). β-actin was used as loading control.

Fig. 4. Unsupervised hierarchical clustering of the 19 genes differentially expressed in HNF1α-mutated HCA that are related to their steatotic phenotype. The dendrogram was obtained based on the expression profile of quantitative RT-PCR data. Samples and genes were classified using the dChip 1.3 software and Pearson correlation algorithm. The data are shown in a table format in which rows represent individual gene and columns represent individual tissue. Red and green colors indicate transcript expression levels respectively above and below the mean (black) expression value for each gene across the entire set of tissue samples.

Fig. 5. Quantification of total fatty acids and neutral lipids. All the results are expressed as mean ± SD. * difference between groups at $P<0.05$. **A.** Total fatty acids (FA) content**. B.** Ratio of total fatty acids**. C.** SFA quantification**. D.** MUFA quantification**. E.** PUFA quantification**. F.** Quantification of neutral lipids classes, CE: cholesterol esters, DG: diglycerides, TG: triglycerides **. G.** Measurement of triglyceride families defined according to their total number of carbon atoms.

Fig. 6. Expression of transcription factors involved in the regulation of liver glucido-lipidic metabolism. A. mRNA level was assessed using quantitative RT-PCR. Results are expressed as the n-fold difference in gene expression relative to the mean expression value of non-tumor livers. Data are mean ± SD. *, **, *** difference between groups at $P<0.05$, 0.01, and 0.001 respectively**. B.** Protein level of SREBP-1 (precursor form 125 kDa and mature form 68 kDa) and ChREBP (95 kDa) were analysed by western-blotting in total and nuclear protein fraction from 3 HNF1α-mutated HCA (T_1, T_2, T_3) and their respective corresponding non-tumor liver (N_1, N_2, N_3) ; the expression level of FAS (265 kDa) and GK (52 kDa) proteins, two targets of SREBP-1 and ChREBP was also assessed in the total protein fraction from the same samples. β-actin and Lamin A/C were used as loading controls for total and nuclear extracts respectively.

Table 1. Quantification of phospholipid classes.

	Non-tumor livers[a]	HNF1α-mutated HCA[b]	Non-tumor livers	HNF1α-mutated HCA
	(pmol/mg of protein)		(% of total phospholipids)	
Total PL	392.13 ± 75.35	**868.38 ± 234.67*** **		
PC	215.55 ± 57.87	**418.92 ± 98.32*** **	55.21 ± 10.84	48.68 ± 4.06
PE	131.26 ± 41.33	**385.76 ± 119*** **	33.07 ± 9.78	**44.23 ± 4.64***
PI	18.44 ± 4.66	29.92 ± 15.41	4.74 ± 0.93	**3.32 ± 1.07***
PS	3.5 ± 6.49	nd	0.97 ± 1.8	nd
SM	23.18 ± 12.4	33.89 ± 25.52	6.01 ± 3.2	3.77 ± 2.88

PL: phospholipids. Values are mean ± SD. nd: not detected. *, *** difference between groups at $P<0.05$ and 0.001 respectively. [a]n=8, [b]n=8

Table 2. Fatty acid composition in each class of phospholipid.

	Total PL		**PC**		**PE**		**PS-PI**	
% of total fatty acids	Non-tumor livers[a]	HNF1α-mutated HCA[b]	Non-tumor livers	HNF1α-mutated HCA	Non-tumor livers	HNF1α-mutated HCA	Non-tumor livers	HNF1α-mutated HCA
SFA	49.13 ± 1.18	46.61 ± 1.75	47.96 ± 1.7	**44.66 ± 0.99***	48.96 ± 1.12	47.34 ± 3.26	54.15 ± 4.36	56.08 ± 3.07
MUFA	10.71 ± 1.39	10.31 ± 1.41	13.33 ± 2.01	11.48 ± 1.75	7.84 ± 0.75	8.16 ± 1.81	7.66 ± 0.95	**11.99 ± 0.68***
PUFA	40.16 ± 1.96	43.08 ± 1.97	38.71 ± 2.3	**43.86 ± 2.19***	43.2 ± 1.6	44.5 ± 3.17	38.19 ± 5	31.93 ± 2.57
MUFA/PUFA	0.27 ± 0.04	0.24 ± 0.04	0.35 ± 0.07	0.26 ± 0.05	0.18 ± 0.02	0.18 ± 0.04	0.21 ± 0.05	**0.38 ± 0.02***
MUFA/SFA	0.22 ± 0.03	0.22 ± 0.03	0.28 ± 0.05	0.26 ± 0.04	0.16 ± 0.01	0.17 ± 0.05	0.14 ± 0.01	**0.21 ± 0.02***
SFA/PUFA	1.23 ± 0.08	1.08 ± 0.09	1.24 ± 0.10	**1.02 ± 0.07***	1.14 ± 0.07	1.07 ± 0.15	1.45 ± 0.32	1.77 ± 0.25
SFA/UFA	0.97 ± 0.05	0.87 ± 0.06	0.92 ± 0.06	**0.81 ± 0.03***	0.96 ± 0.04	0.90 ± 0.12	1.20 ± 0.22	1.29 ± 0.17
C14-C18/C20-C24	3.11 ± 0.49	**2.18 ± 0.28***	5.26 ± 1.04	**2.87 ± 0.46***	1.85 ± 0.29	1.48 ± 0.2	2.42 ± 0.59	2.46 ± 0.4
UI	1.48 ± 0.11	1.70 ± 0.12	1.27 ± 0.10	**1.55 ± 0.08***	1.81 ± 0.11	1.97 ± 0.22	1.46 ± 0.21	1.40 ± 0.11

Values are mean ± SD. UI, Unsaturation index=Σ (% each unsaturated fatty acid x number of double bonds of the same fatty acid)/100. * difference between groups at $P<0.05$. [a]n=4, [b]n=5

Figure 1

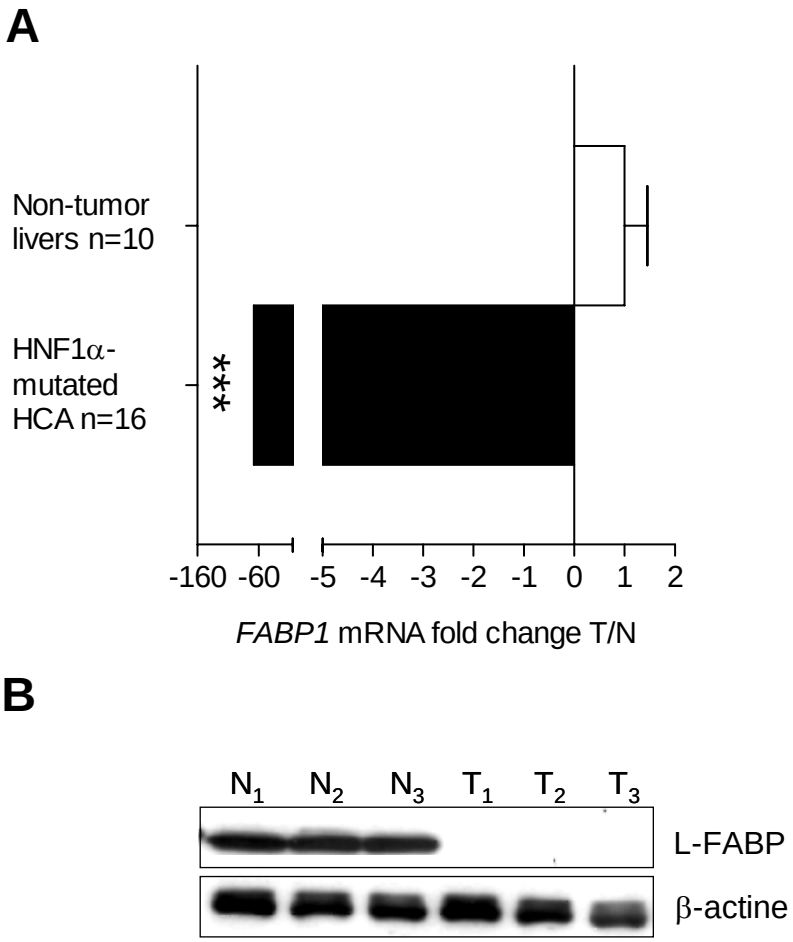

Figure 2

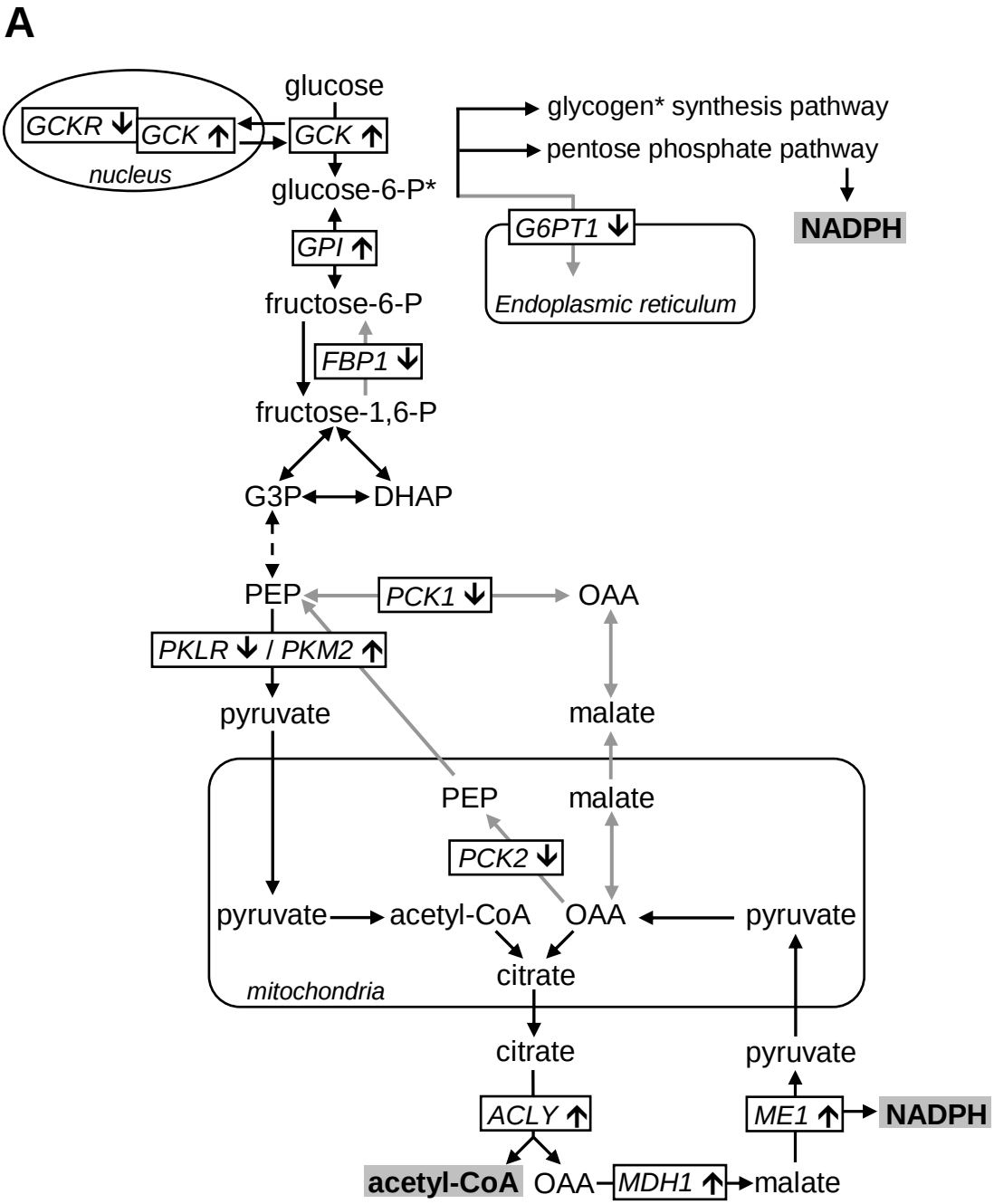

Figure 2

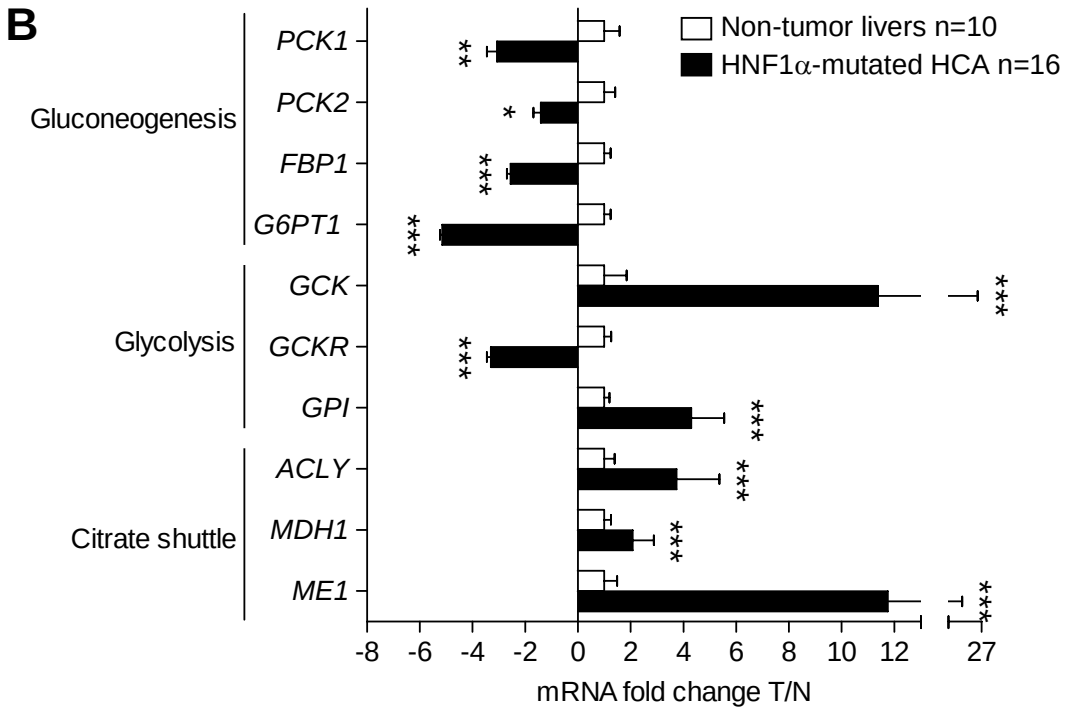

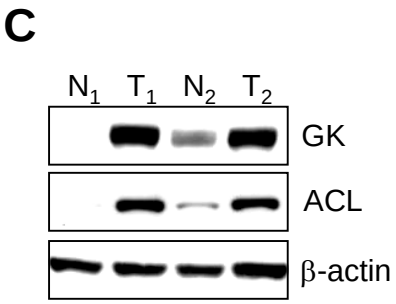

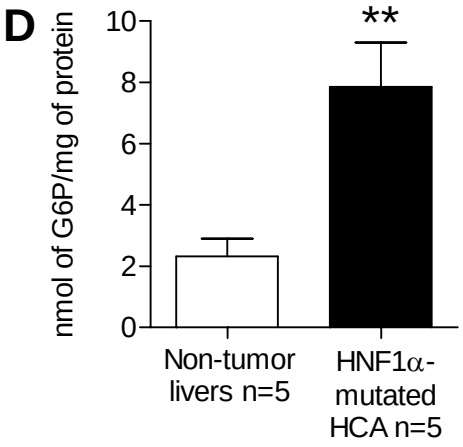

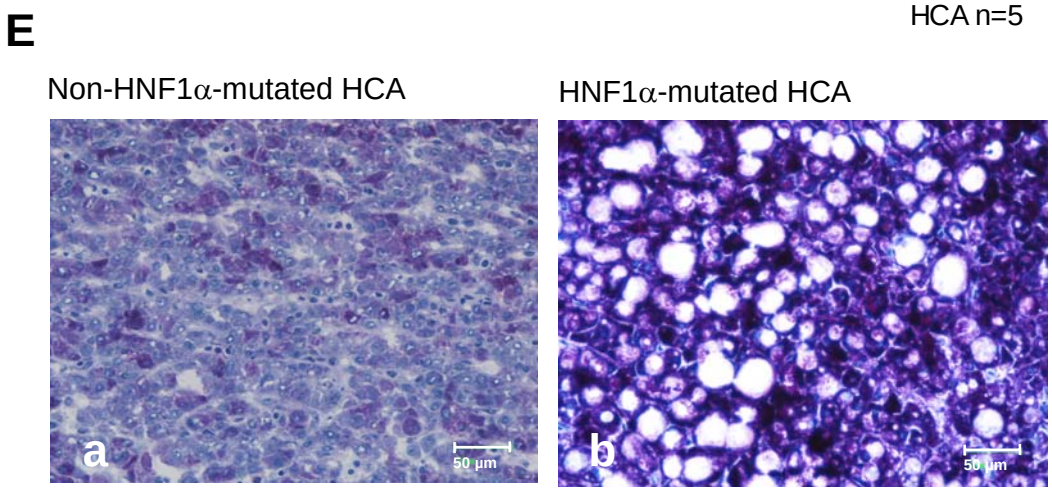

Figure 2

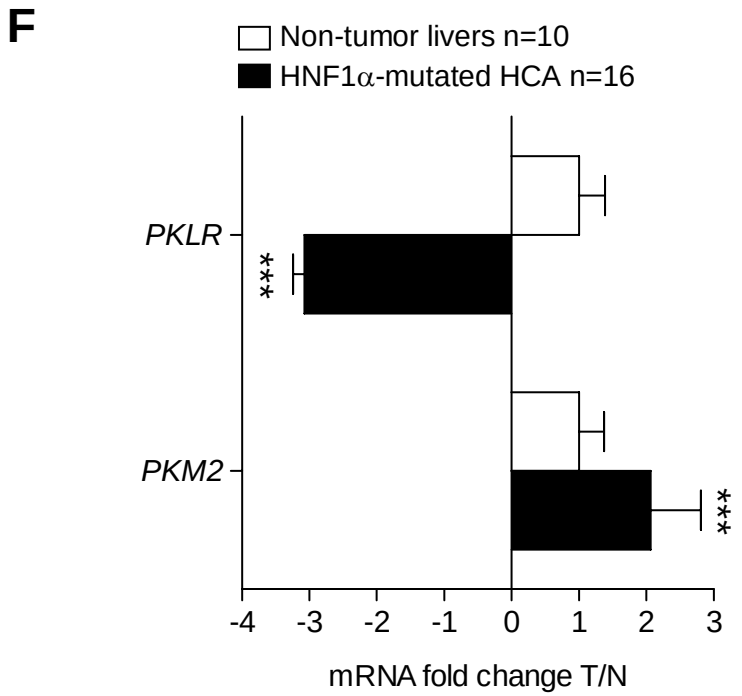

Figure 3

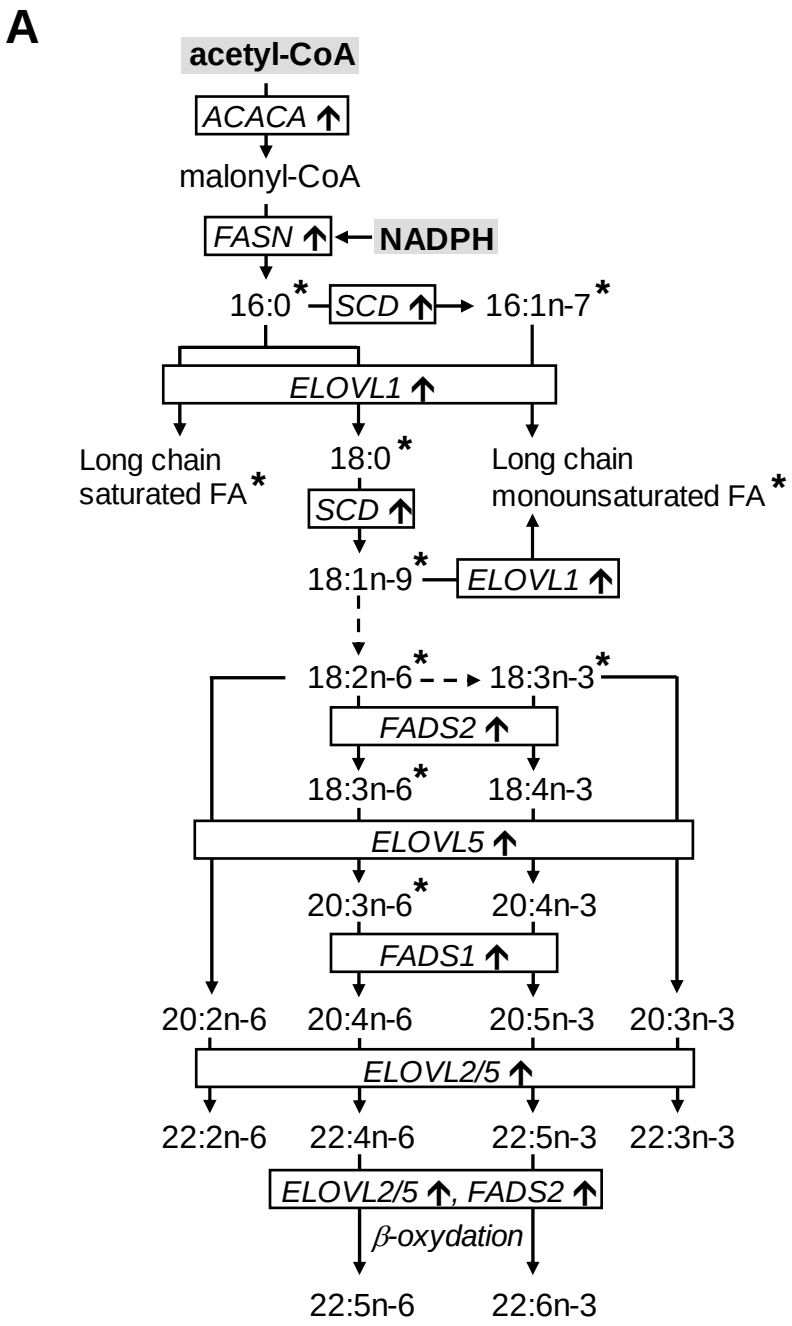

Figure 3

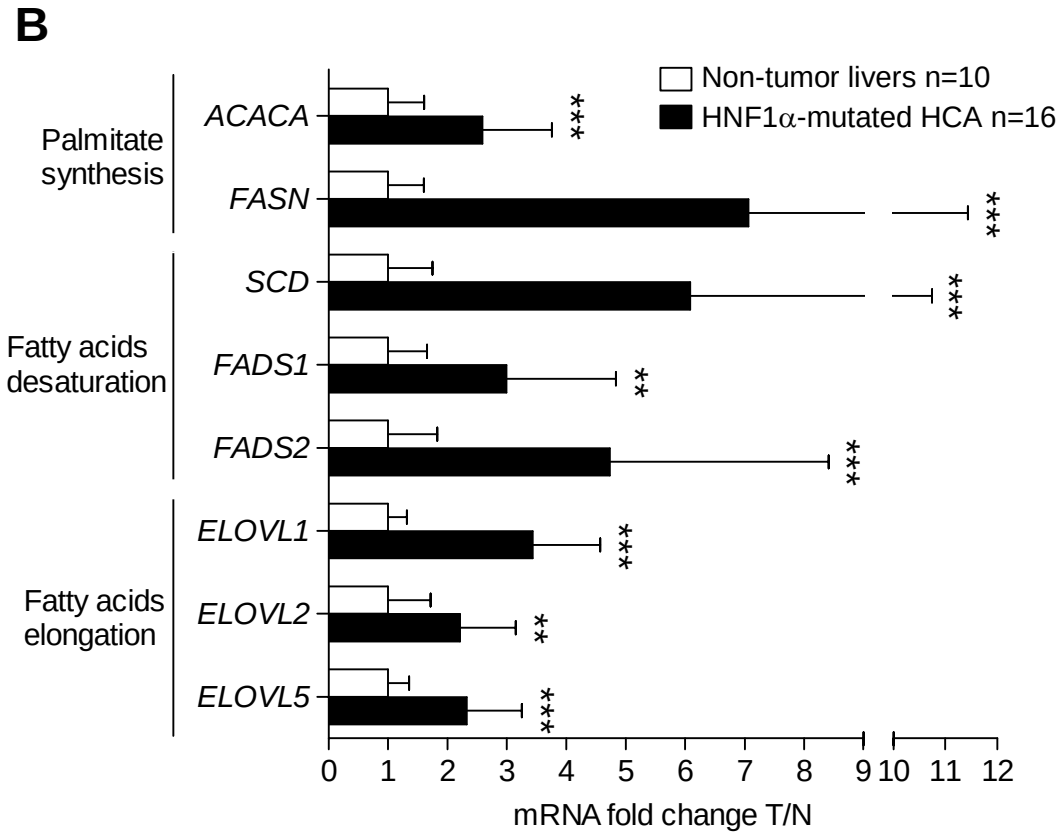

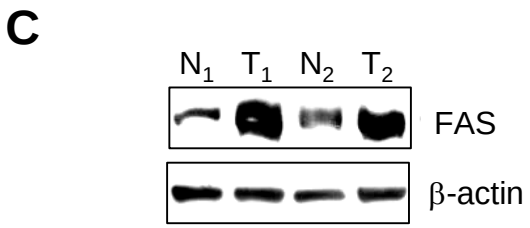

Figure 4

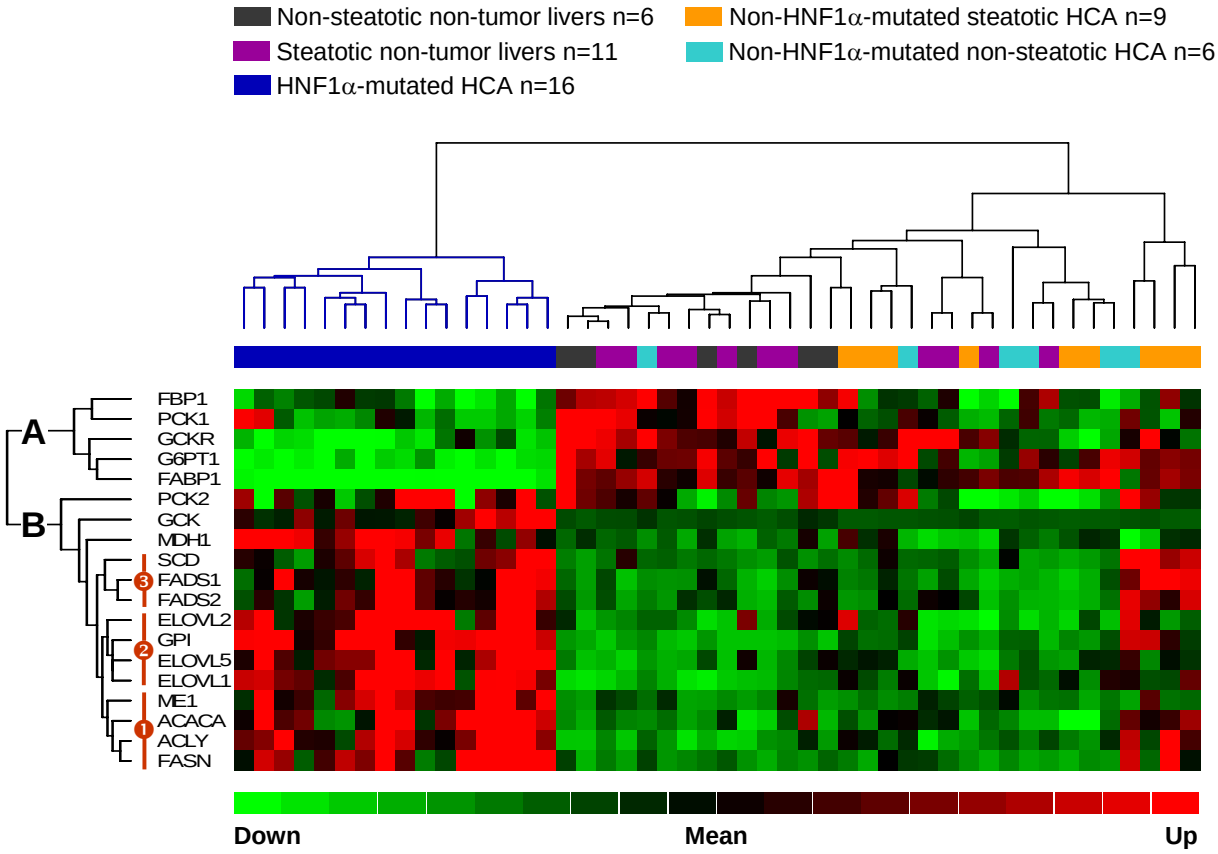

Figure 5

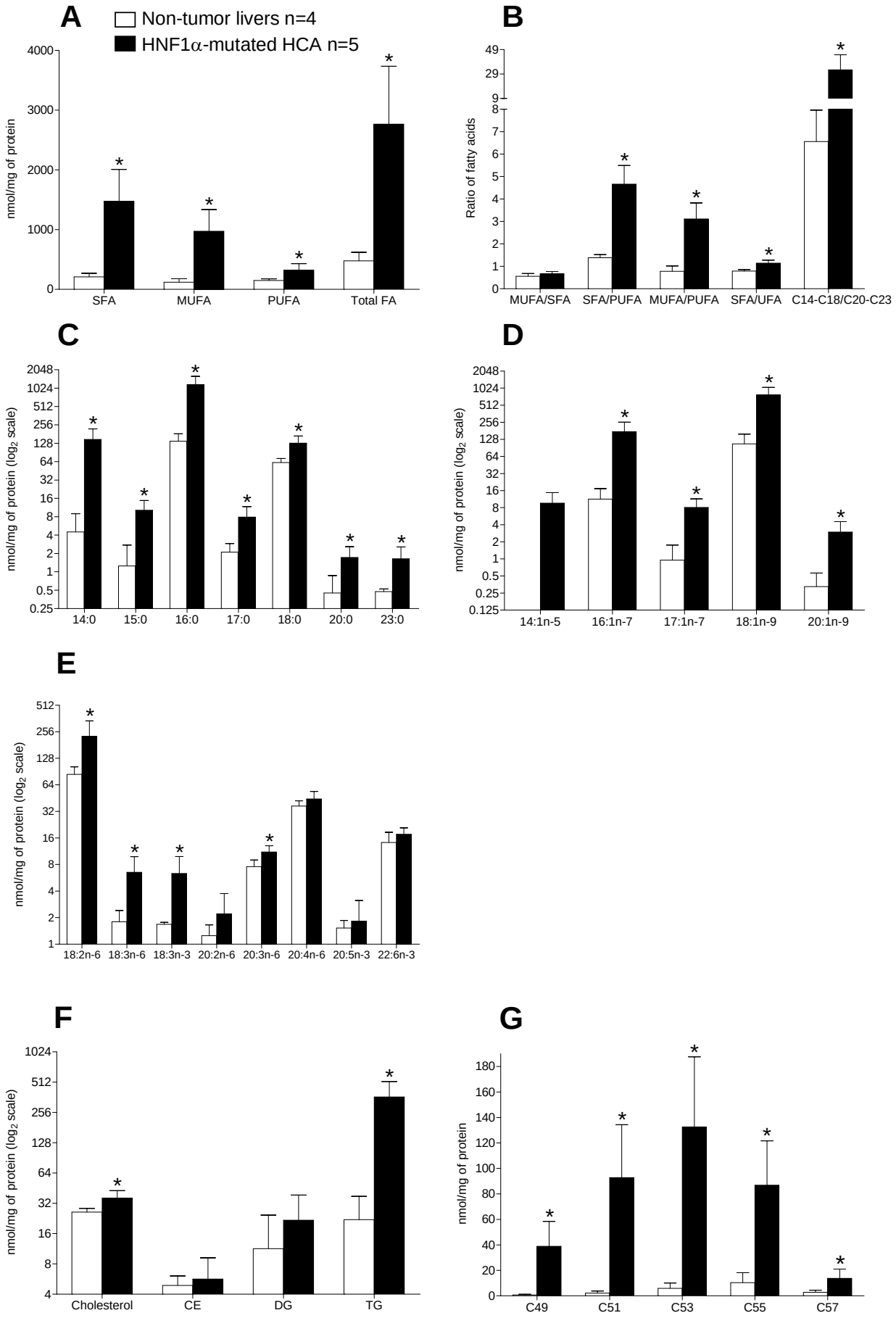

Figure 6

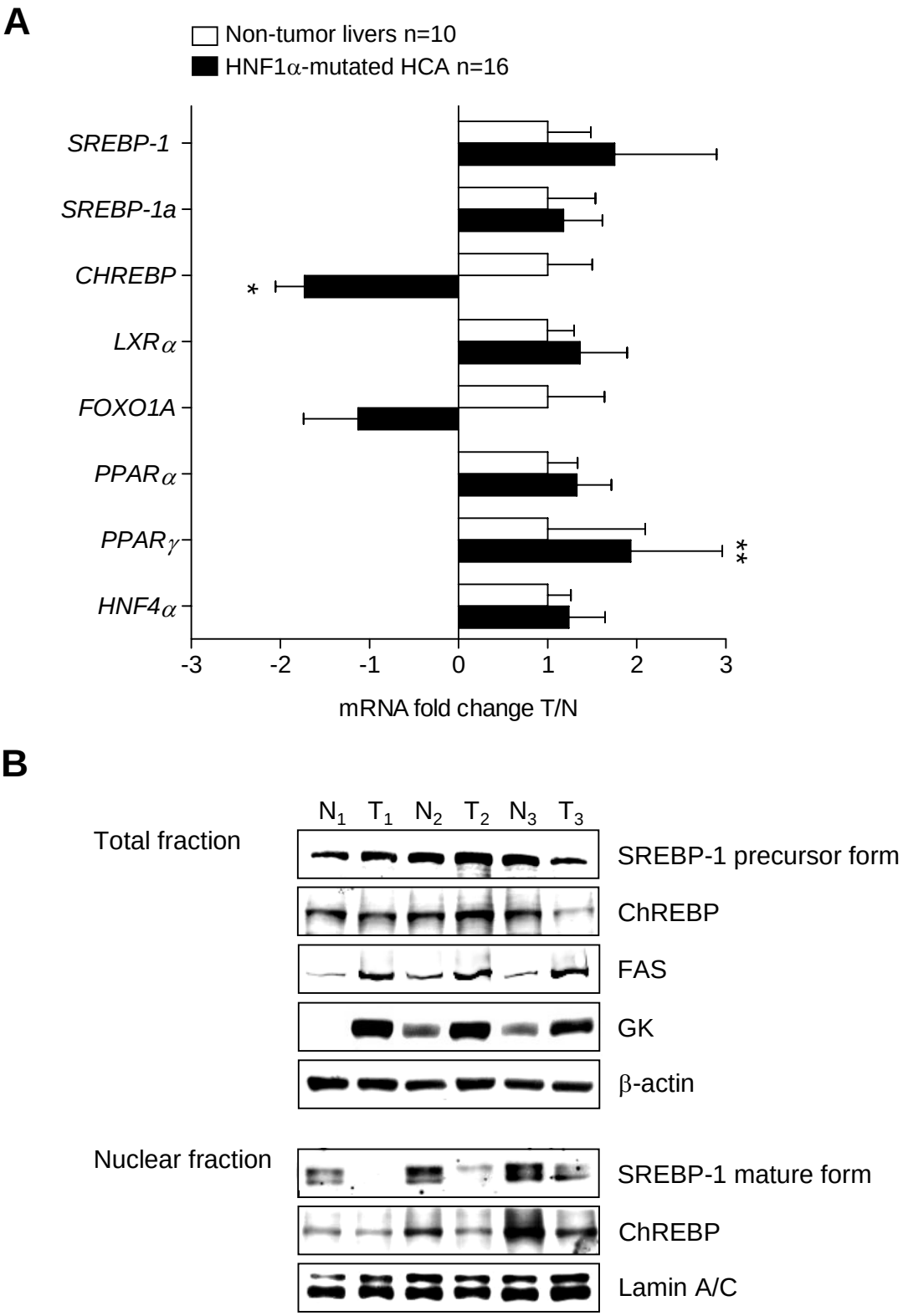

SUPPLEMENTAL DATA

Supplemental experimental procedures

Microarray analysis. In a first experiment, expression patterns were compared between 8 HNF1α-mutated HCA and their corresponding non-tumor livers using cDNA *in-house* manufactured arrays previously described (1). Briefly, one microgram of each amplified RNA and human universal reference RNA (Stratagene) were labeled alternatively with Cy5-dCTP and Cy3-dCTP and co-hybridized onto glass array slides containing 11,250 cDNA spotted sequences. We carried out two hybridizations for each tissue using a dye-swap strategy. Primary data collection, filtering and normalization of gene expression were done as described in Graudens *et al*, (1).

In the second experiment, we used HG-U133A Affymetrix GeneChip™ arrays to compare the expression profiles of 5 HNF1α-mutated HCA and 4 non-related non-tumor livers analysing the expression level of 19,787 probe sets.

Statistical analysis of both cDNA and Affymetrix GeneChip arrays data was performed using multiple testing procedures to evaluate statistical significance for differentially expressed genes, as previously described (1). Two gene selection methods were applied (i) significance analysis of microarrays [SAM; (2)], and (ii) *p*-value ranking using *z*-statistics in ArrayStat 1.0 software (Imaging Research Inc.), *t*-statistics via the dChip program and the class comparison tools available in BRB-ArrayTools v3.2.3 package, an Excel Add-in (3). Statistical tests were computed for each probe set using the log-transformed data and a probe set was declared to be significant when the *p*-value was less than the α-level=0.001. For multiple testing corrections, the false discovery rate (FDR) procedure was used (4). Univariate and multivariate permutation tests (n>1000) were computed to control the proportion of false discoveries (i.e. false positives, > 90% confidence) in the "discovery list". To assess the classification accuracy, a variety of methods were used in BRB-ArrayTools v3.2.3 package, including unsupervised compound covariate, diagonal linear discriminant analysis, k-nearest-neighbor (k=1 and 3), nearest centroid, and support vector machine predictors. For all of those class prediction methods, the cross-validated misclassification rate was calculated using the leave-one-out voting classifier validation (α-level=0.001).

Lipid profiling. Following homogenization of tissue samples in methanol/ 5mM EGTA (2:1 v/v), lipids corresponding to an equivalent of 1 mg of tissue were extracted according to Bligh and Dyer (5) in chloroform/methanol/water (2.5 :2.5 :2.1, v/v/v), in the presence of the internal standards : 6 µg of stigmasterol, 4 µg of 1,3-dimyristine, 4 µg of cholesteryl heptadecanoate and 6 µg of glyceryl triheptadecanoate. Neutral lipids were analyzed by gas-liquid chromatography on a FOCUS Thermo Electron system using a Zebron-1 Phenomenex fused silica capillary columns (5m X 0,32mm i.d, 0.50 mm film thickness) (6). Oven temperature was programmed from 200°C to 350°C at a rate of 5°C per min and the carrier gas was hydrogen (0.5 bar). The injector and the detector were at 315°C and 345°C respectively.

To measure total fatty acid methyl ester molecular species (FAME), lipids corresponding to an equivalent of 1mg of liver were extracted in the presence of glyceryl triheptadecanoate (0.5µg) as an internal standard. The lipid extract was transmethylated with 1ml of acetyl chloride in methanol (1 /20, v/v) for 90 min at 55°C, evaporated to dryness and the FAMEs were extracted with hexane/water 1:1. The organic phase was evaporated to dryness and dissolved in 50µl ethyl acetate. 1µl of FAME was analyzed by gas-liquid chromatography (7) on a 5890 Hewlett Packard system using a Famewax RESTEK fused silica capillary columns (30 m x 0.32 mm i.d, 0.25 mm film thickness). Oven temperature was programmed from 110°C to 220°C at a rate of 2°C per min and the carrier gas was hydrogen (0.5 bar). The injector and the detector were at 225°C and 245°C respectively.

Measurement of fatty acid methyl ester molecular species of phospholipids was performed using lipid extract corresponding to an equivalent of 5 mg of liver. Phospholipids were separated by Thin Layer Chromatography in chloroform:methanol:water:acetic acid (65:43:3:1). Standards were run in parallel, stained with iodine and phospholipids spots were identified, scrapped and eluted three times with 1ml of chloroform:methanol (2:1). Extracts from PC, PS-PI and PE were evaporated to

dryness and transmethylated in the presence of nonadecanoic acid (2 µg). FAMEs were extracted in hexane, re-dissolved in 20µl of ethyl acetate and analysed as above.

To measure phospholipid classes, lipids corresponding to an equivalent of 2 mg of liver were extracted. The lipid extract was dissolved in 40 µl of chloroform and 20µl was analysed by HPLC on a Summit DIONEX system using a Uptisphere 6OH (5µm) 250 X 2mm column. The flow rate was 0.2 ml/min and the column temperature was kept at 35°C during all runs. A light-scattering detector was used for the detection (Polymer Laboratories PL-ELS2100). The evaporator and nebulisator temperature was 80°C, and nitrogen pressure was 1.2 ml/min. A ternary solvent system was used: A, isopropanol; B, hexane; C, water. Triethylamine (0.08%, v/v) and acetic acid (1%, v/v) were added to the solvents. The column was equilibrated in 60% B and 2% C and the sample was injected Then the gradient was moved to 49% B and 5,6% C in 23 min and to 0% B and 14% C in 7 min. Finally the gradient was returned to the starting conditions in 10 min and the column was equilibrated for 45min before next run.

1. Graudens, E., Boulanger, V., Mollard, C., Mariage-Samson, R., Barlet, X., Gremy, G., Couillault, C., Lajemi, M., Piatier-Tonneau, D., Zaborski, P., Eveno, E., Auffray, C., and Imbeaud, S. (2006) *Genome Biol* **7**(3), R19
2. Tusher, V. G., Tibshirani, R., and Chu, G. (2001) *Proc Natl Acad Sci U S A* **98**(9), 5116-5121
3. Korn, E. L., McShane, L. M., Troendle, J. F., Rosenwald, A., and Simon, R. (2002) *Br J Cancer* **86**(7), 1093-1096
4. Benjamini, Y., and Hochberg, Y. (1995) *J Roy Stat Soc Series B-Methodological* **57**, 289-300
5. Bligh, E. G., and Dyer, W. J. (1959) *Can J Biochem Physiol* **37**(8), 911-917
6. Barrans, A., Collet, X., Barbaras, R., Jaspard, B., Manent, J., Vieu, C., Chap, H., and Perret, B. (1994) *J Biol Chem* **269**(15), 11572-11577
7. Lillington, J. M., Trafford, D. J., and Makin, H. L. (1981) *Clin Chim Acta* **111**(1), 91-98

Supplemental Tables and Figures

Supplemental Fig 1. Correlations between overexpressed transcripts of the lipogenesis pathway identified in HNF1α-mutated HCA. A. Correlations for each upregulated transcript *versus* the other indicated upregulated transcripts were assessed by Spearman's rank correlation test using the quantitative RT-PCR data obtained in the group of HNF1α-mutated HCA. *, **, *** difference between groups at $P<0.05$, 0.01, and 0.001 respectively (significant correlations are highlighted in black)**.** ns: correlation is not significant. B. Example of graphical representation of significant correlations identified between *FASN*, *ACLY* and *ACACA* transcripts, three key genes of the lipogenesis pathway.

Supplemental Fig 2. Expression of the 19 differentially expressed genes that may explain steatosis in HNF1α-mutated HCA, in other subtypes of liver tissues with or without steatosis. mRNA level was assessed using quantitative RT-PCR. For each group of samples, results are expressed as the n-fold difference in gene expression relative to the mean expression value of non-steatotic non-tumor livers. Data are mean ± SD. *, **, *** difference between groups at $P<0.05$, 0.01, and 0.001 respectively**.**

Supplemental Fig 3. Expression of SREBP-1, ChREBP, FAS and GK proteins in HNF1α-mutated HCA and in non-HNF1α-mutated non-steatotic HCA. SREBP-1 (precursor form 125 kDa and mature form 68 kDa) and ChREBP (95 kDa) expression was analyzed by western-blotting in total and nuclear protein fraction from three additional cases of HNF1α-mutated HCA (T_4, T_5, T_6) and their respective corresponding non-tumor liver (N_4, N_5, N_6), as well as in three non-HNF1α-mutated non-steatotic HCA (T_7, T_8, T_9) and their respective corresponding non-tumor liver (N_7, N_8, N_9). The expression level of FAS (265 kDa) and GK (52 kDa) proteins, two targets of SREBP-1 and ChREBP was also assessed in the total protein fraction from the same samples. β-actin and Lamin A/C were used as loading controls for total and nuclear extracts respectively.

Supplemental Fig 4. Model of the hypothetical mechanisms by which HNF1α may control lipogenic gene expression. A. Direct mechanism: HNF1α may act as a direct repressor of lipogenic genes promoter activity, through direct DNA binding or by interacting with an unknown activator transcription factor or co-activator proteins (A). B. Indirect mechanism: 1) HNF1α may activate the transcription of a repressor protein (R) involved in the promoter repression of lipogenic genes 2) HNF1α may repress the expression of an activator protein (A) involved in the transcriptional activation of the lipogenic genes expression.

Supplemental Table 1. Results from cDNA and Affymetrix microarray experiments comparing respectively 8 HNF1α-mutated HCA to their matched non-tumor livers (N), and five HNF1α-mutated HCA to four non-related non-tumor livers.
Data are expressed as the n-fold difference in gene expression in HNF1 α-mutated HCA (T) relative to non-tumor livers (N). Genes commonly deregulated in *hnf1 α*-null mice (+) includes primarily data extracted from the transcriptional profiling analysis performed by Shih *et al.* in the liver from *hnf1 α*-null mice and others previous candidate gene approach studies, red and green colors indicate respectively genes whose expression was found upregulated and downregulated in the liver from *hnf1 α*-null mice. (x) indicates genes whose promoter region was previously identified by Odom *et al.* to bind HNF1α in primary human hepatocytes, using ChIP.

			Fold change T/N		Genes commonly deregulated in *hnf1 α*- null mice	Genes commonly deregulated in *hnf1 α*-null mice related to glucido-lipidic metabolism	ChIP Odom *et al.*, 2004
Ensembl Gene ID	**Gene Symbol**	**Gene Name**	**cDNA**	**Affymetrix**			
ENSG00000167910	CYP7A1	Cytochrome P450, family 7, subfamily A, polypeptide 1		17,6	+	bile acid synthesis	
ENSG00000084453	SLCO1A2	Solute carrier organic anion transporter family, member 1A2		4,5	+	bile acid transporter	
ENSG00000104549	SQLE	Squalene epoxidase		4,3	+	cholesterol synthesis	
ENSG00000113161	HMGCR	3-hydroxy-3-methylglutaryl-Coenzyme A reductase		2,7	+	cholesterol synthesis	
ENSG00000160285	LSS	Lanosterol synthase (2,3-oxidosqualene-lanosterol cyclase)		2,0	+	cholesterol synthesis	
ENSG00000065833	ME1	Malic enzyme 1, NADP(+)-dependent, cytosolic		5,9	+	citrate shuttle	
ENSG00000134824	FADS2	Fatty acid desaturase 2		3,3	+	fatty acid synthesis	
ENSG00000169710	FASN	Fatty acid synthase	2,3	3,0	+	fatty acid synthesis	
ENSG00000197977	ELOVL2	Elongation of very long chain fatty acids (FEN1/Elo2, SUR4/Elo3, yeast)-like 2		2,5	+	fatty acid synthesis	
ENSG00000099194	SCD	Stearoyl-CoA desaturase (delta-9-desaturase)		2,1	+	fatty acid synthesis	
ENSG00000170323	FABP4	Fatty acid binding protein 4, adipocyte		5,3	+	fatty acid traffiking	
ENSG00000105220	GPI	Glucose phosphate isomerase	1,8	2,1	+	glycolysis	
ENSG00000111666	CHPT1	Choline phosphotransferase 1		1,9	+	phospholipid synthesis	
ENSG00000137700	SLC37A4	Solute carrier family 37 (glycerol-6-phosphate transporter), member 4	-2,7	-3,8	+	gluconeogenesis	
ENSG00000166035	LIPC	Lipase, hepatic		-9,4	+	lipoprotein catabolism	
ENSG00000111964	APOM	Apolipoprotein M		-22,8	+	lipoprotein metabolism	
ENSG00000163586	FABP1	Fatty acid binding protein 1, liver		-500,0	+	fatty acid traffiking	
ENSG00000111700	SLCO1B3	Solute carrier organic anion transporter family, member 1B3		-87,6	+	bile acid transporter	
ENSG00000131910	NR0B2	Nuclear receptor subfamily 0, group B, member 2		-2,4	+	bile acid metabolism	x
ENSG00000113600	C9	Complement component 9		-1000,0	+		
ENSG00000132693	CRP	C-reactive protein, pentraxin-related	-4,3	-666,7	+		x
ENSG00000165841	CYP2C19	Cytochrome P450, family 2, subfamily C, polypeptide 19		-126,9	+		
ENSG00000145826	LECT2	Leukocyte cell-derived chemotaxin 2		-55,6	+		
ENSG00000126838	PZP	Pregnancy-zone protein		-38,5	+		x
ENSG00000148702	HABP2	Hyaluronan binding protein 2		-26,5	+		x
ENSG00000130649	CYP2E1	Cytochrome P450, family 2, subfamily E, polypeptide 1		-26,3	+		
ENSG00000168679	SLC16A4	Solute carrier family 16 (monocarboxylic acid transporters), member 4	-1,5	-15,3	+		
ENSG00000132703	APCS	Amyloid P component, serum	-4,6	-14,3	+		x
ENSG00000160932	LY6E	Lymphocyte antigen 6 complex, locus E		-12,3	+		x
ENSG00000196083	IL1RAP	Interleukin 1 receptor accessory protein		-10,8	+		

ENSG00000065154	OAT	Ornithine aminotransferase (gyrate atrophy)		-10,8	+		
ENSG00000112299	VNN1	Vanin 1		-10,5	+		
ENSG00000164825	DEFB1	Defensin, beta 1		-10,3	+		
ENSG00000055957	ITIH1	Inter-alpha (globulin) inhibitor H1		-9,5	+		
ENSG00000079557	AFM	Afamin		-9,0	+		
ENSG00000185187	SIGIRR	Single Ig IL-1R-related molecule	-3,6	-8,9	+		
ENSG00000149124	GLYAT	Glycine-N-acyltransferase	-4,1	-8,7	+		
ENSG00000116791	CRYZ	Crystallin, zeta (quinone reductase)		-8,4	+		
ENSG00000170099	SERPINA6	Serine (or cysteine) proteinase inhibitor, clade A (alpha-1 antiproteinase, antitrypsin), member 6		-8,2	+		x
ENSG00000140505	CYP1A2	Cytochrome P450, family 1, subfamily A, polypeptide 2		-7,8	+		
ENSG00000135220	FLJ21934	Hypothetical protein FLJ21934		-6,5	+		x
ENSG00000138115	CYP2C8	Cytochrome P450, family 2, subfamily C, polypeptide 8	-2,7	-5,4	+		
ENSG00000154153	FLJ20152	Hypothetical protein FLJ20152		-5,2	+		
ENSG00000021488	SLC7A9	Solute carrier family 7 (cationic amino acid transporter, y+ system), member 9		-4,5	+		
ENSG00000143278	F13B	Coagulation factor XIII, B polypeptide		-4,3	+		
ENSG00000104870	FCGRT	Fc fragment of IgG, receptor, transporter, alpha		-4,2	+		
ENSG00000181784	RNASE4	Angiogenin, ribonuclease, RNase A family, 5	-1,8	-4,1	+		
ENSG00000170095	GK	Glycerol kinase		-3,7	+		
ENSG00000117594	HSD11B1	Hydroxysteroid (11-beta) dehydrogenase 1		-3,7	+		x
ENSG00000136960	ENPP2	Ectonucleotide pyrophosphatase/phosphodiesterase 2 (autotaxin)		-3,5	+		
ENSG00000151790	TDO2	Tryptophan 2,3-dioxygenase	-3,7	-3,5	+		
ENSG00000080166	DCT	Dopachrome tautomerase (dopachrome delta-isomerase, tyrosine-related protein 2)		-3,5	+		
ENSG00000170095	GKP3	Glycerol kinase pseudogene 3		-3,3	+		
ENSG00000115290	GRB14	Growth factor receptor-bound protein 14		-3,2	+		
ENSG00000086696	HSD17B2	Hydroxysteroid (17-beta) dehydrogenase 2	-1,8	-3,1	+		x
ENSG00000120833	SOCS2	Suppressor of cytokine signaling 2	-1,7	-2,8	+		
ENSG00000118514	ALDH8A1	Aldehyde dehydrogenase 8 family, member A1		-2,8	+		
ENSG00000160282	FTCD	Formiminotransferase cyclodeaminase		-2,7	+		
ENSG00000132541	HRSP12	Heat-responsive protein 12		-2,6	+		
ENSG00000171759	PAH	Phenylalanine hydroxylase		-2,6	+		
ENSG00000188313	PLSCR1	Phospholipid scramblase 1		-2,5	+		
ENSG00000144035	CML2	Putative N-acetyltransferase Camello 2		-2,4	+		
ENSG00000017427	IGF1	Insulin-like growth factor 1 (somatomedin C)	-2,2	-2,4	+		
ENSG00000107554	DNMBP	Dynamin binding protein		-2,3	+		
ENSG00000139547	RODH-4	Microsomal NAD+-dependent retinol dehydrogenase 4		-2,2	+		
ENSG00000112964	GHR	Growth hormone receptor		-2,2	+		
ENSG00000172828	FLJ21736	Esterase 31		-2,2	+		
ENSG00000015475	BID	BH3 interacting domain death agonist	-1,3	-2,2	+		
ENSG00000122194	PLG	Plasminogen		-2,0	+		x

ENSG00000118271	TTR	Transthyretin (prealbumin, amyloidosis type I)		-1,8	+		
ENSG00000176890	TYMS	Thymidylate synthetase	1,6	1,8	+		
ENSG00000146701	MDH2	Malate dehydrogenase 2, NAD (mitochondrial)	1,3	1,9	+		
ENSG00000197448	GSTK1	Glutathione S-transferase kappa 1		1,9	+		
ENSG00000164089	AGXT2L1	Alanine-glyoxylate aminotransferase 2-like 1		1,9	+		
ENSG00000135002	RFK	Riboflavin kinase		2,0	+		
ENSG00000169903	TM4SF4	Transmembrane 4 L six family member 4		2,1	+		x
ENSG00000198638	HLA-B	Major histocompatibility complex, class I, B		2,3	+		
ENSG00000112186	CAP2	CAP, adenylate cyclase-associated protein, 2 (yeast)	1,4	2,7	+		
ENSG00000187837	HIST1H1C	Histone 1, H1c	2,1	2,7	+		
ENSG00000124107	SLPI	Secretory leukocyte protease inhibitor (antileukoproteinase)		3,2	+		x
ENSG00000182718	ANXA2	Annexin A2	1,6	3,4	+		
ENSG00000169245	CXCL10	Chemokine (C-X-C motif) ligand 10		4,0	+		
ENSG00000075142	SRI	Sorcin		2,0			x
ENSG00000106105	GARS	Glycyl-tRNA synthetase	2,2				x
ENSG00000151632	AKR1C2	Aldo-keto reductase family 1, member C2 (dihydrodiol dehydrogenase 2; bile acid binding protein; 3-alpha hydroxysteroid dehydrogenase, type III)		-1,9			x
ENSG00000137106	GRHPR	Glyoxylate reductase/hydroxypyruvate reductase	-1,6	-2,0			x
ENSG00000166825	ANPEP	Alanyl (membrane) aminopeptidase (aminopeptidase N, aminopeptidase M, microsomal aminopeptidase, CD13, p150)		-2,5			x
ENSG00000084734	GCKR	Glucokinase (hexokinase 4) regulator		-3,7			x
ENSG00000165272	AQP3	Aquaporin 3		-3,8			x
ENSG00000198610	AKR1C4	Aldo-keto reductase family 1, member C4 (chlordecone reductase; 3-alpha hydroxysteroid dehydrogenase, type I; dihydrodiol dehydrogenase 4)		-4,6			x
ENSG00000114771	AADAC	Arylacetamide deacetylase (esterase)		-5,3			x
ENSG00000116833	NR5A2	Nuclear receptor subfamily 5, group A, member 2		-5,4			x
ENSG00000187193	MT1X	Metallothionein 1X		-5,4			x
ENSG00000198417	MT1H	Metallothionein 1H	-2,9	-5,6			x
ENSG00000123838	C4BPA	Complement component 4 binding protein, alpha		-5,7			x
ENSG00000172955	ADH6	Alcohol dehydrogenase 6 (class V)		-6,6			x
ENSG00000023839	ABCC2	ATP-binding cassette, sub-family C (CFTR/MRP), member 2		-7,3			x
ENSG00000021461	CYP3A43	Cytochrome P450, family 3, subfamily A, polypeptide 43		-15,4			x
ENSG00000112337	SLC17A2	Solute carrier family 17 (sodium phosphate), member 2		-19,7			x
ENSG00000176153	GPX2	Glutathione peroxidase 2 (gastrointestinal)	-3,9	-20,7			x
ENSG00000109758	HGFAC	HGF activator		-27,3			x
ENSG00000125551	PLGL	Plasminogen-like B1	-2,7				x
ENSG00000125144	MT1G	Metallothionein 1G	-9,8	-6,8			

ENSG00000134538	SLCO1B1	Solute carrier organic anion transporter family, member 1B1	-9,3	-14,7			
ENSG00000172345	STARD5	START domain containing 5	-9,3	-2,5			
ENSG00000132437	DDC	Dopa decarboxylase (aromatic L-amino acid decarboxylase)	-8,0	-10,5			
ENSG00000135069	PSAT1	Phosphoserine aminotransferase 1	-6,4	-11,4			
ENSG00000100558	PLEK2	Pleckstrin 2	-5,9	-2,6			
ENSG00000160868	CYP3A4	Cytochrome P450, family 3, subfamily A, polypeptide 4	-4,5	-73,7			
ENSG00000005187	SAH	SA hypertension-associated homolog (rat)	-4,3	-100,7			
ENSG00000128266	GNAZ	Guanine nucleotide binding protein (G protein), alpha z polypeptide	-4,2				
ENSG00000116717	GADD45A	Growth arrest and DNA-damage-inducible, alpha	-4,0				
ENSG00000092621	PHGDH	Phosphoglycerate dehydrogenase	-3,8	-5,1			
ENSG00000134470	IL15RA	Interleukin 15 receptor, alpha	-3,8				
ENSG00000102078	SLC25A14	Solute carrier family 25 (mitochondrial carrier, brain), member 14	-3,7				
ENSG00000109667	SLC2A9	Solute carrier family 2 (facilitated glucose transporter), member 9	-3,3				
ENSG00000136689	IL1RN	Interleukin 1 receptor antagonist	-3,3	-3,0			
ENSG00000127666	TRIF	TIR domain containing adaptor inducing interferon-beta	-3,2				
ENSG00000145022	TCTA	T-cell leukemia translocation altered gene	-3,1				
ENSG00000170345	FOS	V-fos FBJ murine osteosarcoma viral oncogene homolog	-3,1	-2,9			
ENSG00000123454	DBH	Dopamine beta-hydroxylase (dopamine beta-monooxygenase)	-3,1				
ENSG00000130600	H19	H19, imprinted maternally expressed untranslated mRNA	-3,1				
ENSG00000131043	C20orf4	Chromosome 20 open reading frame 4	-3,0				
ENSG00000010256	UQCRC1	Ubiquinol-cytochrome c reductase core protein I	-2,9				
ENSG00000171791	BCL2	B-cell CLL/lymphoma 2	-2,9				
ENSG00000166741	NNMT	Nicotinamide N-methyltransferase	-2,7	-4,2			
ENSG00000070087	PFN2	Profilin 2	-2,6	-2,8			
ENSG00000196286		Monoclonal antibody HW1 immunoglobulin light chain variable region	-2,4				
ENSG00000104490	NCALD	Neurocalcin delta	-2,4	-2,7			
ENSG00000171557	FGG	Fibrinogen, gamma polypeptide	-2,4				
ENSG00000159423	ALDH4A1	Aldehyde dehydrogenase 4 family, member A1	-2,4	-3,7			
ENSG00000077782	FGFR1	Fibroblast growth factor receptor 1 (fms-related tyrosine kinase 2, Pfeiffer syndrome)	-2,4				
ENSG00000104760	FGL1	Fibrinogen-like 1	-2,3				
ENSG00000125148	MT2A	Metallothionein 2A	-2,3	-3,8			
ENSG00000096087	GSTA2	Glutathione S-transferase A2	-2,3				
ENSG00000189221	MAOA	Monoamine oxidase A	-2,3	-3,0			
ENSG00000148842	CNNM2	Cyclin M2	-2,2				
ENSG00000087086	FTL	Ferritin, light polypeptide	-2,2	-2,0			
ENSG00000171564	FGB	Fibrinogen, B beta polypeptide	-2,2	-20,0			
ENSG00000121690	LOC91614	Novel 58.3 KDA protein	-2,2				

ENSG00000085999	RAD54L	RAD54-like (S. cerevisiae)	-2,2				
ENSG00000138794	CASP6	Caspase 6, apoptosis-related cysteine protease	-2,1				
ENSG00000146918	MTB	Leucine zipper protein 5	-2,1				
ENSG00000160310	HRMT1L1	HMT1 hnRNP methyltransferase-like 1 (S. cerevisiae)	-2,1				
ENSG00000119686	C14orf58	Chromosome 14 open reading frame 58	-2,1				
ENSG00000092529	CAPN3	Calpain 3, (p94)	-2,0	-3,6			
ENSG00000064995	TAF11	TAF11 RNA polymerase II, TATA box binding protein (TBP)-associated factor, 28kDa	-2,0				
ENSG00000120896	SCAM-1	Vinexin beta (SH3-containing adaptor molecule-1)	-2,0	-1,6			
ENSG00000130707	ASS	Argininosuccinate synthetase	-2,0	-2,5			
ENSG00000161267	BDH	3-hydroxybutyrate dehydrogenase (heart, mitochondrial)	-2,0	-3,6			
ENSG00000177885	GRB2	Growth factor receptor-bound protein 2	-2,0				
ENSG00000115414	FN1	Fibronectin 1	-2,0	-4,7			
ENSG00000107745	CBARA1	Calcium binding atopy-related autoantigen 1	-2,0	-2,8			
ENSG00000153707	PTPRD	Protein tyrosine phosphatase, receptor type, D	-2,0	-2,3			
ENSG00000182979	MTA1	Metastasis associated 1	-2,0				
ENSG00000102401	ARMCX3	Armadillo repeat containing, X-linked 3	-1,9	-1,4			
ENSG00000157353	FUK	Fucokinase	-1,9				
ENSG00000095203	EPB41L4B	Erythrocyte membrane protein band 4.1 like 4B	-1,9	-2,7			
ENSG00000104635	SLC39A14	Solute carrier family 39 (zinc transporter), member 14	-1,9	-2,0			
ENSG00000198270	LOC89894	Hypothetical protein BC000282	-1,9				
ENSG00000163710	PCOLCE2	Procollagen C-endopeptidase enhancer 2	-1,9				
ENSG00000106333	PCOLCE	Procollagen C-endopeptidase enhancer	-1,9				
ENSG00000119938	PPP1R3C	Protein phosphatase 1, regulatory (inhibitor) subunit 3C	-1,9				
ENSG00000198960	ARMCX6	Armadillo repeat containing, X-linked 6	-1,9				
ENSG00000145020	AMT	Aminomethyltransferase (glycine cleavage system protein T)	-1,9				
ENSG00000119711	ALDH6A1	Aldehyde dehydrogenase 6 family, member A1	-1,9	-2,4			
ENSG00000177853	ZNF518	Zinc finger protein 518	-1,8				
ENSG00000116044	NFE2L2	Nuclear factor (erythroid-derived 2)-like 2	-1,8	-1,8			
ENSG00000169692	AGPAT2	1-acylglycerol-3-phosphate O-acyltransferase 2 (lysophosphatidic acid acyltransferase, beta)	-1,8	-3,0			
ENSG00000007565	DAXX	Death-associated protein 6	-1,8				
ENSG00000113269	RNF130	Ring finger protein 130	-1,8	-2,4			
ENSG00000143369	ECM1	Extracellular matrix protein 1	-1,8	-3,3			
ENSG00000162595	ARHI	DIRAS family, GTP-binding RAS-like 3	-1,8	-2,3			
ENSG00000125740	FOSB	FBJ murine osteosarcoma viral oncogene homolog B	-1,7	-3,2			
ENSG00000148672	GLUD1	Glutamate dehydrogenase 1	-1,7	-2,9			
ENSG00000100292	HMOX1	Heme oxygenase (decycling) 1	-1,7	-5,2			
ENSG00000164039	DHRS6	Dehydrogenase/reductase (SDR family) member 6	-1,7	-2,6			

ENSG00000169136	ATF5	Activating transcription factor 5	-1,6	-2,7			
ENSG00000156298	TM4SF2	Tetraspanin 7	-1,6	-2,3			
ENSG00000100814	CCNB1IP1	Cyclin B1 interacting protein 1	-1,6	-4,2			
ENSG00000066468	FGFR2	Fibroblast growth factor receptor 2 (bacteria-expressed kinase, keratinocyte growth factor receptor, craniofacial dysostosis 1, Crouzon syndrome, Pfeiffer syndrome, Jackson-Weiss syndrome)	-1,6	-2,2			
ENSG00000171617	ENC1	Ectodermal-neural cortex (with BTB-like domain)	-1,6	-1,9			
ENSG00000133639	BTG1	B-cell translocation gene 1, anti-proliferative	-1,6	-2,1			
ENSG00000010810	FYN	FYN oncogene related to SRC, FGR, YES	-1,6	-3,6			
ENSG00000117009	KMO	Kynurenine 3-monooxygenase (kynurenine 3-hydroxylase)	-1,5	-3,3			
ENSG00000171793	CTPS	CTP synthase	-1,5	-4,4			
ENSG00000116741	RGS2	Regulator of G-protein signalling 2, 24kDa	-1,5	-2,5			
ENSG00000159674	SPON2	Spondin 2, extracellular matrix protein	-1,5	-2,0			
ENSG00000182551	MTCBP-1	Membrane-type 1 matrix metalloproteinase cytoplasmic tail binding protein-1	-1,5	-1,8			
ENSG00000100897	WDR23	WD repeat domain 23	-1,5	-1,8			
ENSG00000162433	AK3	Adenylate kinase 3-like 1	-1,4	-2,2			
ENSG00000142192	APP	Amyloid beta (A4) precursor protein (protease nexin-II, Alzheimer disease)	-1,4	-2,6			
ENSG00000125520	SLC2A4RG	SLC2A4 regulator	-1,4	-2,2			
ENSG00000109971	HSPA1B	Heat shock 70kDa protein 1B	-1,4	-2,8			
ENSG00000065057	NTHL1	Nth endonuclease III-like 1 (E. coli)	-1,4	-2,6			
ENSG00000123843	C4BPB	Complement component 4 binding protein, beta	-1,4	-2,1			
ENSG00000109861	CTSC	Cathepsin C	-1,4	-2,2			
ENSG00000188042	ARL7	ADP-ribosylation factor-like 7	-1,4	-2,4			
ENSG00000091490	KIAA0746	KIAA0746 protein	-1,3	-2,0			
ENSG00000178980	SEPW1	Selenoprotein W, 1	-1,3	-2,3			
ENSG00000130475	FCHO1	FCH domain only 1	-1,3	-8,9			
ENSG00000137124	ALDH1B1	Aldehyde dehydrogenase 1 family, member B1	-1,3	-3,2			
ENSG00000197451	HNRPAB	Heterogeneous nuclear ribonucleoprotein A/B	1,2	1,8			
ENSG00000106992	AK1	Adenylate kinase 1	1,3	3,4			
ENSG00000158864	NDUFS2	NADH dehydrogenase (ubiquinone) Fe-S protein 2, 49kDa (NADH-coenzyme Q reductase)	1,3	1,9			
ENSG00000105953	OGDH	Oxoglutarate (alpha-ketoglutarate) dehydrogenase (lipoamide)	1,3	2,0			
ENSG00000182054	IDH2	Isocitrate dehydrogenase 2 (NADP+), mitochondrial	1,3	1,9			
ENSG00000161013	MGAT4B	Mannosyl (alpha-1,3-)-glycoprotein beta-1,4-N-acetylglucosaminyltransferase, isoenzyme B	1,3	2,0			
ENSG00000101940	WDR13	WD repeat domain 13	1,3	2,1			
ENSG00000138073	PREB	Prolactin regulatory element binding	1,4	2,2			
ENSG00000121054	NME2	Non-metastatic cells 2, protein (NM23B) expressed in	1,4	1,9			
ENSG00000103528	LOC51760	B/K protein	1,4	7,2			

ENSG00000185275	CD24	CD24 antigen (small cell lung carcinoma cluster 4 antigen)	1,4	3,6			
ENSG00000110092	CCND1	Cyclin D1 (PRAD1: parathyroid adenomatosis 1)	1,4	3,6			
ENSG00000161011	SQSTM1	Sequestosome 1	1,4	2,4			
ENSG00000100504	PYGL	Phosphorylase, glycogen; liver (Hers disease, glycogen storage disease type VI)	1,4	2,2			
ENSG00000166971	FTS	Fused toes homolog (mouse)	1,4	2,1			
ENSG00000117984	CTSD	Cathepsin D (lysosomal aspartyl protease)	1,4	2,0			
ENSG00000172115	CYCS	Cytochrome c, somatic	1,4	2,0			
ENSG00000125166	GOT2	Glutamic-oxaloacetic transaminase 2, mitochondrial (aspartate aminotransferase 2)	1,4	2,1			
ENSG00000148334	PTGES2	Prostaglandin E synthase 2	1,4	2,0			
ENSG00000064601	PPGB	Protective protein for beta-galactosidase (galactosialidosis)	1,4	1,9			
ENSG00000113645	KIBRA	KIBRA protein	1,4	2,2			
ENSG00000178558	CRI1	CREBBP/EP300 inhibitor 1	1,4	2,1			
ENSG00000159840	ZYX	Zyxin	1,4	1,8			
ENSG00000120837	NFYB	Nuclear transcription factor Y, beta	1,4	2,2			
ENSG00000002822	MAD1L1	MAD1 mitotic arrest deficient-like 1 (yeast)	1,5	3,3			
ENSG00000071051	NCK2	NCK adaptor protein 2	1,5	3,4			
ENSG00000091409	ITGA6	Integrin, alpha 6	1,5	2,0			
ENSG00000164120	HPGD	Hydroxyprostaglandin dehydrogenase 15-(NAD)	1,5	2,9			
ENSG00000066322	ELOVL1	Elongation of very long chain fatty acids (FEN1/Elo2, SUR4/Elo3, yeast)-like 1	1,5	2,0			
ENSG00000137403	HLA-F	Major histocompatibility complex, class I, F	1,5	2,1			
ENSG00000139641	MBC2	Family with sequence similarity 62 (C2 domain containing), member A	1,5	1,8			
ENSG00000198479	HLA-C	Major histocompatibility complex, class I, C	1,5	2,4			
ENSG00000110955	ATP5B	ATP synthase, H+ transporting, mitochondrial F1 complex, beta polypeptide	1,6	2,1			
ENSG00000145545	SRD5A1	Steroid-5-alpha-reductase, alpha polypeptide 1 (3-oxo-5 alpha-steroid delta 4-dehydrogenase alpha 1)	1,6	1,8			
ENSG00000138074	SLC5A6	Solute carrier family 5 (sodium-dependent vitamin transporter), member 6	1,6	2,5			
ENSG00000119782	FKBP1B	FK506 binding protein 1B, 12.6 kDa	1,7	69,0			
ENSG00000131473	ACLY	ATP citrate lyase	1,7	2,5			
ENSG00000137259	HIST1H2AC	Histone 1, H2ac	1,8	3,3			
ENSG00000131759	RARA	Retinoic acid receptor, alpha	1,8	1,9			
ENSG00000124120	C20orf121	Chromosome 20 open reading frame 121	1,8	2,9			
ENSG00000138131	LOXL4	Lysyl oxidase-like 4	1,8				
ENSG00000144063	BENE	BENE protein	1,8	3,7			
ENSG00000143333	RGS16	Regulator of G-protein signalling 16	1,8	1,7			
ENSG00000068793	CYFIP2	Cytoplasmic FMR1 interacting protein 2	1,8	4,9			
ENSG00000130305	NSUN5	NOL1/NOP2/Sun domain family, member 5	1,8				
ENSG00000120708	TGFBI	Transforming growth factor, beta-induced, 68kDa	1,9	4,6			
ENSG00000164830	OXR1	Oxidation resistance 1	1,9				
ENSG00000115129	TP53I3	Tumor protein p53 inducible protein 3	1,9	4,9			
ENSG00000147065	MSN	Moesin	2,0	2,0			

ENSG00000013364	MVP	Major vault protein	2,0	2,7			
ENSG00000165731	RET	Ret proto-oncogene (multiple endocrine neoplasia and medullary thyroid carcinoma 1, Hirschsprung disease)	2,1	4,4			
ENSG00000103042	FLJ10815	Amino acid transporter	2,1	2,7			
ENSG00000132329	RAMP1	Receptor (calcitonin) activity modifying protein 1	2,2	2,8			
ENSG00000129116	KIAA0992	Palladin	2,3	3,7			
ENSG00000028310	BRD9	Bromodomain containing 9	2,3				
ENSG00000112293	GPLD1	Glycosylphosphatidylinositol specific phospholipase D1	2,7	5,1			
ENSG00000130294	KIF1A	Kinesin family member 1A	2,7				
ENSG00000134769	DTNA	Dystrobrevin, alpha	2,9	2,2			
ENSG00000049759	NEDD4L	Neural precursor cell expressed, developmentally down-regulated 4-like	3,2	3,7			
ENSG00000160097	FNDC5	Fibronectin type III domain containing 5	3,3				
ENSG00000008517	NK4	Interleukin 32	3,4				
ENSG00000115875	SFRS7	Splicing factor, arginine/serine-rich 7, 35kDa	7,1				
ENSG00000171819	ANGPTL7	Angiopoietin-like 7	10,0				
ENSG00000160870	CYP3A7	Cytochrome P450, family 3, subfamily A, polypeptide 7		-1138,6			
ENSG00000080345	RIF1	RAP1 interacting factor homolog (yeast)		-538,1			
ENSG00000123561	SERPINA7	Serine (or cysteine) proteinase inhibitor, clade A (alpha-1 antiproteinase, antitrypsin), member 7		-500,0			
ENSG00000169688	MT1K	Metallothionein 1K		-131,3			
ENSG00000175003	SLC22A1	Solute carrier family 22 (organic cation transporter), member 1		-86,0			
ENSG00000049883	PTCD2	Pentatricopeptide repeat domain 2		-79,3			
ENSG00000168259	DNAJC7	DnaJ (Hsp40) homolog, subfamily C, member 7		-70,0			
ENSG00000167165	UGT1A6	UDP glycosyltransferase 1 family, polypeptide A9		-45,9			
ENSG00000114200	BCHE	Butyrylcholinesterase		-39,9			
ENSG00000129214	SHBG	Sex hormone-binding globulin		-27,8			
ENSG00000158296	SLC13A3	Solute carrier family 13 (sodium-dependent dicarboxylate transporter), member 3		-24,9			
ENSG00000124713	GNMT	Glycine N-methyltransferase		-24,4			
ENSG00000127831	VIL1	Villin 1		-23,8			
ENSG00000100665	SERPINA4	Serine (or cysteine) proteinase inhibitor, clade A (alpha-1 antiproteinase, antitrypsin), member 4		-22,8			
ENSG00000160867	FGFR4	Fibroblast growth factor receptor 4		-21,7			
ENSG00000160339	FCN2	Ficolin (collagen/fibrinogen domain containing lectin) 2 (hucolin)		-20,8			
ENSG00000157399	ARSE	Arylsulfatase E (chondrodysplasia punctata 1)		-20,8			
ENSG00000173930	SLCO4C1	Solute carrier organic anion transporter family, member 4C1		-20,4			
ENSG00000164711	LPAL2	Lipoprotein, Lp(a)-like 2		-19,6			
ENSG00000105701	FKBP8	FK506 binding protein 8, 38kDa		-19,3			
ENSG00000091972	CD200	CD200 antigen		-19,2			
ENSG00000125144	MT1F	Metallothionein 1F (functional)		-19,2			
ENSG00000108187	MAWBP	MAWD binding protein		-19,1			

ENSG00000138079	SLC3A1	Solute carrier family 3 (cystine, dibasic and neutral amino acid transporters, activator of cystine, dibasic and neutral amino acid transport), member 1		-18,1			
ENSG00000183682	BMP8A	Bone morphogenetic protein 8a		-17,5			
ENSG00000080709	KCNN2	Potassium intermediate/small conductance calcium-activated channel, subfamily N, member 2		-16,2			
ENSG00000086205	FOLH1	Folate hydrolase (prostate-specific membrane antigen) 1		-15,2			
ENSG00000174156	GSTA3	Glutathione S-transferase A3		-15,0			
ENSG00000138109	CYP2C9	Cytochrome P450, family 2, subfamily C, polypeptide 9		-14,4			
ENSG00000108231	LGI1	Leucine-rich, glioma inactivated 1		-13,5			
ENSG00000163032	VSNL1	Visinin-like 1		-13,3			
ENSG00000104938	CD209L	C-type lectin domain family 4, member M		-12,4			
ENSG00000187097	ENTPD5	Ectonucleoside triphosphate diphosphohydrolase 5		-11,6			
ENSG00000009694		CDNA clone IMAGE:4811759, partial cds		-10,6			
ENSG00000115919	KYNU	Kynureninase (L-kynurenine hydrolase)		-10,5			
ENSG00000161270	PRODH2	Proline dehydrogenase (oxidase) 2		-9,3			
ENSG00000135625	EGR4	Early growth response 4		-9,2			
ENSG00000086300	SNX10	Sorting nexin 10		-9,0			
ENSG00000165682	CLEC2	C-type lectin domain family 1, member B		-7,4			
ENSG00000175336	APOF	Apolipoprotein F		-7,2			
ENSG00000067208	EVI5	Ecotropic viral integration site 5		-7,1			
ENSG00000169715	MT1E	Metallothionein 1E (functional)		-6,1			
ENSG00000162545	CaMKIINalpha	Calcium/calmodulin-dependent protein kinase II		-6,1			
ENSG00000138640	FAM13A1	Family with sequence similarity 13, member A1		-5,9			
ENSG00000114115	RBP1	Retinol binding protein 1, cellular		-5,6			
ENSG00000133800	XLKD1	Extracellular link domain containing 1		-5,5			
ENSG00000184292	TACSTD2	Tumor-associated calcium signal transducer 2		-5,4			
ENSG00000102891	MT4	Metallothionein IV		-5,4			
ENSG00000140465	CYP1A1	Cytochrome P450, family 1, subfamily A, polypeptide 1		-5,3			
ENSG00000188257	PLA2G2A	Phospholipase A2, group IIA (platelets, synovial fluid)		-5,2			
ENSG00000159461	AMFR	Autocrine motility factor receptor		-5,2			
ENSG00000139508	LOC283537	Hypothetical protein LOC283537		-5,2			
ENSG00000075340	ADD2	Adducin 2 (beta)		-5,1			
ENSG00000142748	FCN3	Ficolin (collagen/fibrinogen domain containing) 3 (Hakata antigen)		-5,0			
ENSG00000135423	GLS2	Glutaminase 2 (liver, mitochondrial)		-5,0			
ENSG00000136213	CHST12	Carbohydrate (chondroitin 4) sulfotransferase 12		-5,0			
ENSG00000198805	NP	Nucleoside phosphorylase		-4,9			
ENSG00000095596	CYP26A1	Cytochrome P450, family 26, subfamily A, polypeptide 1		-4,9			
ENSG00000090512	FETUB	Fetuin B		-4,4			
ENSG00000198670	LPA	Lipoprotein, Lp(a)		-4,3			

ENSG00000141338	ABCA8	ATP-binding cassette, sub-family A (ABC1), member 8		-4,3			
ENSG00000101057	MYBL2	V-myb myeloblastosis viral oncogene homolog (avian)-like 2		-4,2			
ENSG00000130227	XPO7	Exportin 7		-4,2			
ENSG00000141293	SCAP1	Src family associated phosphoprotein 1		-4,2			
ENSG00000166922	SGNE1	Secretory granule, neuroendocrine protein 1 (7B2 protein)		-4,1			
ENSG00000143627	PKLR	Pyruvate kinase, liver and RBC		-4,1			
ENSG00000124568	SLC17A1	Solute carrier family 17 (sodium phosphate), member 1		-4,1			
ENSG00000134363	FST	Follistatin		-4,0			
ENSG00000110244	APOA4	Apolipoprotein A-IV		-4,0			
ENSG00000101349	PAK7	P21(CDKN1A)-activated kinase 7		-3,9			
ENSG00000189013	KIR2DL4	Killer cell immunoglobulin-like receptor, two domains, long cytoplasmic tail, 4		-3,9			
ENSG00000079805	DNM2	Dynamin 2		-3,8			
ENSG00000153904	DDAH1	Dimethylarginine dimethylaminohydrolase 1		-3,8			
ENSG00000120054	CPN1	Carboxypeptidase N, polypeptide 1, 50kD		-3,8			
ENSG00000136870	ZNF189	Zinc finger protein 189		-3,7			
ENSG00000100031	GGTL4	Gamma-glutamyltransferase-like 4		-3,6			
ENSG00000165507	C10orf10	Chromosome 10 open reading frame 10		-3,5			
ENSG00000189056	RELN	Reelin		-3,5			
ENSG00000143630	HCN3	Hyperpolarization activated cyclic nucleotide-gated potassium channel 3		-3,5			
ENSG00000142494	FLJ10847	Hypothetical protein FLJ10847		-3,4			
ENSG00000155666	FLJ13798	Hypothetical protein FLJ13798		-3,4			
ENSG00000075651	PLD1	Phospholipase D1, phophatidylcholine-specific		-3,4			
ENSG00000101911	PRPS2	Phosphoribosyl pyrophosphate synthetase 2		-3,3			
ENSG00000164647	STEAP	Six transmembrane epithelial antigen of the prostate 1		-3,3			
ENSG00000169032	MAP2K1	Mitogen-activated protein kinase kinase 1		-3,3			
ENSG00000141179	PCTP	Phosphatidylcholine transfer protein		-3,2			
ENSG00000145287	PLAC8	Placenta-specific 8		-3,2			
ENSG00000087237	CETP	Cholesteryl ester transfer protein, plasma		-3,2			
ENSG00000173610	UGT2A1	UDP glycosyltransferase 2 family, polypeptide A1		-3,1			
ENSG00000013016	EHD3	EH-domain containing 3		-3,1			
ENSG00000145824	CXCL14	Chemokine (C-X-C motif) ligand 14		-3,0			
ENSG00000141441	C18orf11	Family with sequence similarity 59, member A		-3,0			
ENSG00000143507	DUSP10	Dual specificity phosphatase 10		-2,9			
ENSG00000070729	CNGB1	Cyclic nucleotide gated channel beta 1		-2,9			
ENSG00000165140	FBP1	Fructose-1,6-bisphosphatase 1		-2,9			
ENSG00000100031	GGT1	Gamma-glutamyltransferase 1		-2,8			
ENSG00000182890	GLUD2	Glutamate dehydrogenase 2		-2,8			
ENSG00000135226	UGT2B28	UDP glycosyltransferase 2 family, polypeptide B28		-2,8			

ENSG00000113196	HAND1	Heart and neural crest derivatives expressed 1		-2,8			
ENSG00000115525	SIAT9	ST3 beta-galactoside alpha-2,3-sialyltransferase 5		-2,8			
ENSG00000137561	TTPA	Tocopherol (alpha) transfer protein (ataxia (Friedreich-like) with vitamin E deficiency)		-2,8			
ENSG00000161574	CCL15	Chemokine (C-C motif) ligand 14		-2,8			
ENSG00000163687	DNASE1L3	Deoxyribonuclease I-like 3		-2,8			
ENSG00000168421	RHOH	Ras homolog gene family, member H		-2,8			
ENSG00000072694	FCGR2B	Fc fragment of IgG, low affinity IIb, receptor (CD32)		-2,7			
ENSG00000159723	AGRP	Agouti related protein homolog (mouse)		-2,7			
ENSG00000092820	VIL2	Villin 2 (ezrin)		-2,7			
ENSG00000131018	SYNE1	Spectrin repeat containing, nuclear envelope 1		-2,6			
ENSG00000108479	GALK1	Galactokinase 1		-2,6			
ENSG00000095739	BAMBI	BMP and activin membrane-bound inhibitor homolog (Xenopus laevis)		-2,6			
ENSG00000185650	ZFP36L1	Zinc finger protein 36, C3H type-like 1		-2,6			
ENSG00000116761	CTH	Cystathionase (cystathionine gamma-lyase)		-2,6			
ENSG00000101856	PGRMC1	Progesterone receptor membrane component 1		-2,6			
ENSG00000165475	CRYL1	Crystallin, lambda 1		-2,6			
ENSG00000139289	PHLDA1	Pleckstrin homology-like domain, family A, member 1		-2,6			
ENSG00000117479	SLC19A2	Solute carrier family 19 (thiamine transporter), member 2		-2,5			
ENSG00000119866	BCL11A	B-cell CLL/lymphoma 11A (zinc finger protein)		-2,5			
ENSG00000010327	STAB1	Stabilin 1		-2,5			
ENSG00000196177	ACADSB	Acyl-Coenzyme A dehydrogenase, short/branched chain		-2,5			
ENSG00000151422	FER	Fer (fps/fes related) tyrosine kinase (phosphoprotein NCP94)		-2,5			
ENSG00000152558	PORIMIN	Pro-oncosis receptor inducing membrane injury gene		-2,4			
ENSG00000103200	NME4	Non-metastatic cells 4, protein expressed in		-2,4			
ENSG00000060762	BRP44L	Brain protein 44-like		-2,4			
ENSG00000175806	MSRA	Methionine sulfoxide reductase A		-2,4			
ENSG00000117983	MUC5AC	Mucin 5, subtypes A and C, tracheobronchial/gastric		-2,4			
ENSG00000129007	CALML4	Calmodulin-like 4		-2,4			
ENSG00000106025	TM4SF12	Tetraspanin 12		-2,4			
ENSG00000096395	MLN	Motilin		-2,4			
ENSG00000185000	DGAT1	Diacylglycerol O-acyltransferase homolog 1 (mouse)		-2,4			
ENSG00000124374	KIAA1155	KIAA1155 protein		-2,4			
ENSG00000114698	PLSCR4	Phospholipid scramblase 4		-2,4			
ENSG00000131171	SH3BGRL	SH3 domain binding glutamic acid-rich protein like		-2,4			
ENSG00000117036	ETV3	Ets variant gene 3		-2,3			
ENSG00000197747	S100A10	S100 calcium binding protein A10 (annexin II ligand, calpactin I, light polypeptide (p11))		-2,3			
ENSG00000135318	NT5E	5'-nucleotidase, ecto (CD73)		-2,3			
ENSG00000144035	NAT8	N-acetyltransferase 8 (camello like)		-2,3			

ENSG00000133983	C14orf112	Chromosome 14 open reading frame 112		-2,3			
ENSG00000132207	SULT1A3	Sulfotransferase family, cytosolic, 1A, phenol-preferring, member 3		-2,3			
ENSG00000138744	ASAHL	N-acylsphingosine amidohydrolase (acid ceramidase)-like		-2,3			
ENSG00000170458	CD14	CD14 antigen		-2,3			
ENSG00000112494	UNC93A	Unc-93 homolog A (C. elegans)		-2,3			
ENSG00000148468	C10orf38	Chromosome 10 open reading frame 38		-2,3			
ENSG00000102897	LOC57149	Hypothetical protein A-211C6.1		-2,3			
ENSG00000071894	CPSF1	Cleavage and polyadenylation specific factor 1, 160kDa		-2,3			
ENSG00000105852	PON3	Paraoxonase 3		-2,3			
ENSG00000137414	FAM8A1	Family with sequence similarity 8, member A1		-2,3			
ENSG00000110011	DNAJC4	DnaJ (Hsp40) homolog, subfamily C, member 4		-2,2			
ENSG00000156113	KCNMA1	Potassium large conductance calcium-activated channel, subfamily M, alpha member 1		-2,2			
ENSG00000112769	LAMA4	Laminin, alpha 4		-2,2			
ENSG00000197114	FLJ20406	Lck interacting transmembrane adaptor 1		-2,2			
ENSG00000083857	FAT	FAT tumor suppressor homolog 1 (Drosophila)		-2,2			
ENSG00000143845	ETNK2	Ethanolamine kinase 2		-2,2			
ENSG00000123500	COL10A1	Collagen, type X, alpha 1(Schmid metaphyseal chondrodysplasia)		-2,2			
ENSG00000100116	GCAT	Glycine C-acetyltransferase (2-amino-3-ketobutyrate coenzyme A ligase)		-2,2			
ENSG00000085465	OVGP1	Oviductal glycoprotein 1, 120kDa (mucin 9, oviductin)		-2,2			
ENSG00000197321	SVIL	Supervillin		-2,1			
ENSG00000176170	SPHK1	Sphingosine kinase 1		-2,1			
ENSG00000197165	SULT1A2	Sulfotransferase family, cytosolic, 1A, phenol-preferring, member 2		-2,1			
ENSG00000101577	LPIN2	Lipin 2		-2,1			
ENSG00000130522	JUND	Jun D proto-oncogene		-2,1			
ENSG00000146674	IGFBP3	Insulin-like growth factor binding protein 3		-2,1			
ENSG00000170430	MGMT	O-6-methylguanine-DNA methyltransferase		-2,1			
ENSG00000137960	GIPC2	PDZ domain protein GIPC2		-2,1			
ENSG00000105711	SCN1B	Sodium channel, voltage-gated, type I, beta		-2,1			
ENSG00000072840	EVC	Ellis van Creveld syndrome		-2,1			
ENSG00000149435	GGTLA4	Gamma-glutamyltransferase-like activity 4		-2,1			
ENSG00000130076	IGHG3	Immunoglobulin heavy constant mu		-2,1			
ENSG00000147394	ZNF185	Zinc finger protein 185 (LIM domain)		-2,1			
ENSG00000160973	FOXH1	Forkhead box H1		-2,1			
ENSG00000169951	MGC13138	Hypothetical protein MGC13138		-2,0			
ENSG00000123496	IL13RA2	Interleukin 13 receptor, alpha 2		-2,0			
ENSG00000152104	PTPN14	Protein tyrosine phosphatase, non-receptor type 14		-2,0			
ENSG00000149084	HSD17B12	Hydroxysteroid (17-beta) dehydrogenase 12		-2,0			
ENSG00000082438	COBLL1	COBL-like 1		-2,0			

ENSG00000182165	TP53AP1	TP53 activated protein 1		-2,0			
ENSG00000173918	C1QTNF1	C1q and tumor necrosis factor related protein 1		-2,0			
ENSG00000137992	DBT	Dihydrolipoamide branched chain transacylase E2		-2,0			
ENSG00000167800	TBX10	T-box 10		-2,0			
ENSG00000159200	DSCR1	Down syndrome critical region gene 1		-2,0			
ENSG00000023330	ALAS1	Aminolevulinate, delta-, synthase 1		-2,0			
ENSG00000160862	AZGP1	Alpha-2-glycoprotein 1, zinc		-2,0			
ENSG00000151224	MAT1A	Methionine adenosyltransferase I, alpha		-2,0			
ENSG00000178075	GRAMD1C	GRAM domain containing 1C		-1,9			
ENSG00000171067	C11orf24	Chromosome 11 open reading frame 24		-1,9			
ENSG00000137642	SORL1	Sortilin-related receptor, L(DLR class) A repeats-containing		-1,9			
ENSG00000197114	ZGPAT	Zinc finger, CCCH-type with G patch domain		-1,9			
ENSG00000166886	NAB2	NGFI-A binding protein 2 (EGR1 binding protein 2)		-1,9			
ENSG00000109814	UGDH	UDP-glucose dehydrogenase		-1,9			
ENSG00000096141	LY6G6D	Chromosome 6 open reading frame 21		-1,9			
ENSG00000142634	EFHD2	EF hand domain family, member D2		-1,9			
ENSG00000143815	LBR	Lamin B receptor		-1,9			
ENSG00000102934	TM4SF11	Plasma membrane proteolipid (plasmolipin)		-1,8			
ENSG00000102010	BMX	BMX non-receptor tyrosine kinase		-1,8			
ENSG00000100321	SYNGR1	Synaptogyrin 1		-1,8			
ENSG00000143793	C1orf35	Chromosome 1 open reading frame 35		-1,8			
ENSG00000178105	DDX10	DEAD (Asp-Glu-Ala-Asp) box polypeptide 10		-1,8			
ENSG00000137699	TRIM29	Tripartite motif-containing 29		-1,8			
ENSG00000140575	IQGAP1	IQ motif containing GTPase activating protein 1		-1,8			
ENSG00000139644	TEGT	Testis enhanced gene transcript (BAX inhibitor 1)		-1,8			
ENSG00000140459	CYP11A1	Cytochrome P450, family 11, subfamily A, polypeptide 1		-1,6			
ENSG00000069966	GNB5	Guanine nucleotide binding protein (G protein), beta 5		1,8			
ENSG00000099290	RP11-56A21.1	Similar to KIAA0592 protein		1,8			
ENSG00000111711	CGI-141	Golgi transport 1 homolog B (S. cerevisiae)		1,8			
ENSG00000122873	C10orf70	Chromosome 10 open reading frame 70		1,8			
ENSG00000136986	DERL1	Der1-like domain family, member 1		1,9			
ENSG00000023228	NDUFS1	NADH dehydrogenase (ubiquinone) Fe-S protein 1, 75kDa (NADH-coenzyme Q reductase)		1,9			
ENSG00000174640	SLCO2A1	Solute carrier organic anion transporter family, member 2A1		1,9			
ENSG00000172731	LRRC20	Leucine rich repeat containing 20		1,9			
ENSG00000143061	IGSF3	Immunoglobulin superfamily, member 3		1,9			
ENSG00000173660	UQCRH	Ubiquinol-cytochrome c reductase hinge protein		1,9			
ENSG00000106052	TAX1BP1	Tax1 (human T-cell leukemia virus type I) binding protein 1		1,9			
ENSG00000178234	GALNT11	UDP-N-acetyl-alpha-D-galactosamine:polypeptide N-acetylgalactosaminyltransferase 11 (GalNAc-T11)		1,9			

ENSG00000111801	BTN3A3	Butyrophilin, subfamily 3, member A3		1,9			
ENSG00000137204	SLC22A7	Solute carrier family 22 (organic anion transporter), member 7		1,9			
ENSG00000113108	APBB3	Amyloid beta (A4) precursor protein-binding, family B, member 3		2,0			
ENSG00000196655	TRAPPC4	Trafficking protein particle complex 4		2,0			
ENSG00000180304	OAZ2	Ornithine decarboxylase antizyme 2		2,0			
ENSG00000109654	TRIM2	Tripartite motif-containing 2		2,0			
ENSG00000108641	EPPB9	B9 protein		2,0			
ENSG00000149485	FADS1	Fatty acid desaturase 1		2,0			
ENSG00000197597	H2BFS	H2B histone family, member S		2,0			
ENSG00000049541	RFC2	Replication factor C (activator 1) 2, 40kDa		2,0			
ENSG00000139190	VAMP1	Vesicle-associated membrane protein 1 (synaptobrevin 1)		2,0			
ENSG00000187758	ADH1C	Alcohol dehydrogenase 1C (class I), gamma polypeptide		2,0			
ENSG00000198793	FRAP1	FK506 binding protein 12-rapamycin associated protein 1		2,0			
ENSG00000196700	SOX18	SRY (sex determining region Y)-box 18		2,1			
ENSG00000125967	APBA2BP	Amyloid beta (A4) precursor protein-binding, family A, member 2 binding protein		2,1			
ENSG00000117289	TXNIP	Thioredoxin interacting protein		2,1			
ENSG00000172292	LASS6	LAG1 longevity assurance homolog 6 (S. cerevisiae)		2,1			
ENSG00000168061	SHD1	SAC3 domain containing 1		2,1			
ENSG00000168899	VAMP5	Vesicle-associated membrane protein 5 (myobrevin)		2,1			
ENSG00000105854	PON2	Paraoxonase 2		2,1			
ENSG00000197635	DPP4	Dipeptidylpeptidase 4 (CD26, adenosine deaminase complexing protein 2)		2,1			
ENSG00000134698	EIF2C4	Eukaryotic translation initiation factor 2C, 4		2,2			
ENSG00000012660	ELOVL5	ELOVL family member 5, elongation of long chain fatty acids (FEN1/Elo2, SUR4/Elo3-like, yeast)		2,2			
ENSG00000137575	SDCBP	Syndecan binding protein (syntenin)		2,2			
ENSG00000140939	NOL3	Nucleolar protein 3 (apoptosis repressor with CARD domain)		2,2			
ENSG00000066044	ELAVL1	ELAV (embryonic lethal, abnormal vision, Drosophila)-like 1 (Hu antigen R)		2,2			
ENSG00000144749	LRIG1	Leucine-rich repeats and immunoglobulin-like domains 1		2,2			
ENSG00000197694	SPTAN1	Spectrin, alpha, non-erythrocytic 1 (alpha-fodrin)		2,2			
ENSG00000186480	INSIG1	Insulin induced gene 1		2,2			
ENSG00000100029	PES1	Pescadillo homolog 1, containing BRCT domain (zebrafish)		2,3			
ENSG00000068745	IHPK2	Inositol hexaphosphate kinase 2		2,3			
ENSG00000138821	SLC39A8	Solute carrier family 39 (zinc transporter), member 8		2,3			
ENSG00000197499	HLA-A	Major histocompatibility complex, class I, A		2,3			

ENSG00000131773	KHDRBS3	KH domain containing, RNA binding, signal transduction associated 3		2,3			
ENSG00000183087	GAS6	Growth arrest-specific 6		2,3			
ENSG00000072042	RDH11	DKFZP564M1462 protein		2,3			
ENSG00000072682	P4HA2	Procollagen-proline, 2-oxoglutarate 4-dioxygenase (proline 4-hydroxylase), alpha polypeptide II		2,3			
ENSG00000133131	ZCWCC2	Zinc finger, CW type with coiled-coil domain 2		2,3			
ENSG00000143643	TTC13	Tetratricopeptide repeat domain 13		2,3			
ENSG00000178878	DKFZP434F0318	Hypothetical protein DKFZp434F0318		2,3			
ENSG00000188126	MYO15B	Myosin XVB, pseudogene		2,3			
ENSG00000188301	PDGFA	Platelet-derived growth factor alpha polypeptide		2,3			
ENSG00000110852	CLECSF2	C-type lectin domain family 2, member B		2,3			
ENSG00000101782	RIOK3	RIO kinase 3 (yeast)		2,3			
ENSG00000176887	SOX11	SRY (sex determining region Y)-box 11		2,3			
ENSG00000138193	PLCE1	Phospholipase C, epsilon 1		2,3			
ENSG00000008283	CYB561	Cytochrome b-561		2,4			
ENSG00000176658	MYO1D	Myosin ID		2,4			
ENSG00000198758	EPS8L3	EPS8-like 3		2,4			
ENSG00000100941	PNN	Pinin, desmosome associated protein		2,4			
ENSG00000025708	ECGF1	Endothelial cell growth factor 1 (platelet-derived)		2,4			
ENSG00000118804	GENX-3414	Genethonin 1		2,4			
ENSG00000113732	ATP6V0E	ATPase, H+ transporting, lysosomal 9kDa, V0 subunit e		2,4			
ENSG00000158321	AUTS2	Autism susceptibility candidate 2		2,4			
ENSG00000140092	FBLN5	Fibulin 5		2,4			
ENSG00000078114	NEBL	Nebulette		2,4			
ENSG00000150403	C13orf11	Chromosome 13 open reading frame 11		2,4			
ENSG00000123240	OPTN	Optineurin		2,5			
ENSG00000124635	HIST1H2BK	Histone 1, H2bk		2,5			
ENSG00000156831	FLJ32440	Hypothetical protein FLJ32440		2,5			
ENSG00000114251	WNT5A	Wingless-type MMTV integration site family, member 5A		2,5			
ENSG00000198586	TLK1	Tousled-like kinase 1		2,5			
ENSG00000075151	EIF4G3	Eukaryotic translation initiation factor 4 gamma, 3		2,5			
ENSG00000011052	NME1	Non-metastatic cells 1, protein (NM23A) expressed in		2,6			
ENSG00000198872	PEG10	Paternally expressed 10		2,6			
ENSG00000050165	DKK3	Dickkopf homolog 3 (Xenopus laevis)		2,6			
ENSG00000140632	N-PAC	Cytokine-like nuclear factor n-pac		2,7			
ENSG00000198722	UNC13B	Unc-13 homolog B (C. elegans)		2,7			
ENSG00000005471	ABCB4	ATP-binding cassette, sub-family B (MDR/TAP), member 4		2,7			
ENSG00000073008	PVR	Poliovirus receptor		2,7			
ENSG00000168242	HIST1H2BH	Histone 1, H2bh		2,8			
ENSG00000149554	CHEK1	CHK1 checkpoint homolog (S. pombe)		2,8			
ENSG00000103657	HERC1	Hect (homologous to the E6-AP (UBE3A) carboxyl terminus) domain and RCC1 (CHC1)-like domain (RLD) 1		2,8			
ENSG00000187164	KIAA1598	KIAA1598		2,9			

ENSG00000136854	STXBP1	Syntaxin binding protein 1		3,0			
ENSG00000101849	TBL1X	Transducin (beta)-like 1X-linked		3,1			
ENSG00000198730	SH2BP1	SH2 domain binding protein 1 (tetratricopeptide repeat containing)		3,1			
ENSG00000129538	RNASE1	Ribonuclease, RNase A family, 1 (pancreatic)		3,2			
ENSG00000141447	OSBPL1A	Oxysterol binding protein-like 1A		3,2			
ENSG00000146904	EPHA1	EPH receptor A1		3,2			
ENSG00000112378	PERP	PERP, TP53 apoptosis effector		3,2			
ENSG00000134324	LPIN1	Lipin 1		3,2			
ENSG00000166033	PRSS11	Protease, serine, 11 (IGF binding)		3,3			
ENSG00000160752	FDPS	Farnesyl diphosphate synthase (farnesyl pyrophosphate synthetase, dimethylallyltranstransferase, geranyltranstransferase)		3,4			
ENSG00000107518	ATRNL1	Attractin-like 1		3,5			
ENSG00000173698	GPR64	G protein-coupled receptor 64		3,5			
ENSG00000100297	MCM5	MCM5 minichromosome maintenance deficient 5, cell division cycle 46 (S. cerevisiae)		3,5			
ENSG00000145730	PAM	Peptidylglycine alpha-amidating monooxygenase		3,6			
ENSG00000196187	TMEM63A	Transmembrane protein 63A		3,6			
ENSG00000141736	ERBB2	V-erb-b2 erythroblastic leukemia viral oncogene homolog 2, neuro/glioblastoma derived oncogene homolog (avian)		3,6			
ENSG00000148180	GSN	Gelsolin (amyloidosis, Finnish type)		3,7			
ENSG00000184115	LOC440895	Similar to LIM and senescent cell antigen-like domains 3		3,8			
ENSG00000184304	PRKD1	Protein kinase D1		4,0			
ENSG00000160202	CRYAA	Crystallin, alpha A		4,2			
ENSG00000162909	CAPN2	Calpain 2, (m/II) large subunit		4,3			
ENSG00000164035	EMCN	Endomucin		4,4			
ENSG00000112320	FLJ10159	Hypothetical protein FLJ10159		4,5			
ENSG00000128284	APOL3	Apolipoprotein L, 3		4,5			
ENSG00000133985	TTC9	Tetratricopeptide repeat domain 9		4,7			
ENSG00000175054	ATR	Ataxia telangiectasia and Rad3 related		4,8			
ENSG00000105499	PLA2G4C	Phospholipase A2, group IVC (cytosolic, calcium-independent)		5,0			
ENSG00000130300	PLVAP	Plasmalemma vesicle associated protein		5,3			
ENSG00000177697	CD151	CD151 antigen		5,3			
ENSG00000047597	XK	Kell blood group precursor (McLeod phenotype)		5,9			
ENSG00000116661	FBXO2	F-box protein 2		6,1			
ENSG00000163993	S100P	S100 calcium binding protein P		8,2			
ENSG00000197402	UBD	Ubiquitin D		8,7			
ENSG00000163923	RPL39L	Ribosomal protein L39-like		8,8			
ENSG00000144476	CMKOR1	Chemokine orphan receptor 1		8,9			
ENSG00000021645	NRXN1	Neurexin 1		9,5			
ENSG00000138028	CGREF1	Cell growth regulator with EF hand domain 1		9,6			
ENSG00000101210	EEF1A2	Eukaryotic translation elongation factor 1 alpha 2		10,6			
ENSG00000148634	HERC4	Hect domain and RLD 4		13,9			

ENSG00000185697	MYBL1	V-myb myeloblastosis viral oncogene homolog (avian)-like 1		15,2			
ENSG00000066279	ASPM	Asp (abnormal spindle)-like, microcephaly associated (Drosophila)		16,6			
ENSG00000198000	NOL8	Nucleolar protein 8		19,6			
ENSG00000204291	COL15A1	Collagen, type XV, alpha 1		25,8			
ENSG00000110799	VWF	Von Willebrand factor		38,2			
ENSG00000100311	PDGFB	Platelet-derived growth factor beta polypeptide (simian sarcoma viral (v-sis) oncogene homolog)		44,0			
ENSG00000133048	CHI3L1	Chitinase 3-like 1 (cartilage glycoprotein-39)		96,3			

Supplemental Figure 1

A

			MDH1	GCK	FADS2	FADS1	SCD	ELOVL1	ELOVL5	GPI	ELOVL2	FASN	ACLY	ACACA
Cluster 1	ME1	Spearman r	ns	ns	0,73	ns	0,64	0,61	0,69	0,58	ns	0,67	0,64	0,55
		P value summary			**		**	*	**	*		**	**	*
	ACACA	Spearman r	ns	ns	ns	ns	ns	ns	0,54	ns	ns	0,72	0,72	
		P value summary							*			**	**	
	ACLY	Spearman r	ns	ns	ns	ns	0,61	0,57	ns	0,56	ns	0,70		
		P value summary					*	*		*		**		
	FASN	Spearman r	ns	ns	ns	ns	0,65	ns	0,58	0,68	ns			
		P value summary					**		*	**				
Cluster 2	ELOVL2	Spearman r	ns	ns	0,61	ns	ns	0,85	0,56	ns				
		P value summary			*			***	*					
	GPI	Spearman r	ns	ns	ns	ns	0,56	ns	0,56					
		P value summary					*		*					
	ELOVL5	Spearman r	ns	ns	0,65	0,56	0,70	0,58						
		P value summary			**	*	**	*						
	ELOVL1	Spearman r	ns	ns	0,58	0,52	ns							
		P value summary			*	*								
Cluster 3	SCD	Spearman r	ns	ns	0,72	ns								
		P value summary			**									
	FADS1	Spearman r	ns	ns	0,70									
		P value summary			**									
	FADS2	Spearman r	ns	ns										
		P value summary												
	GCK	Spearman r	- 0,69											
		P value summary	**											

B

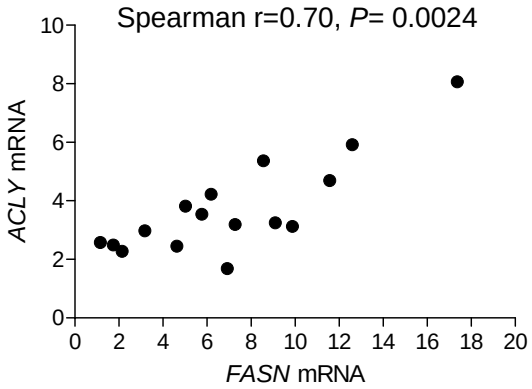

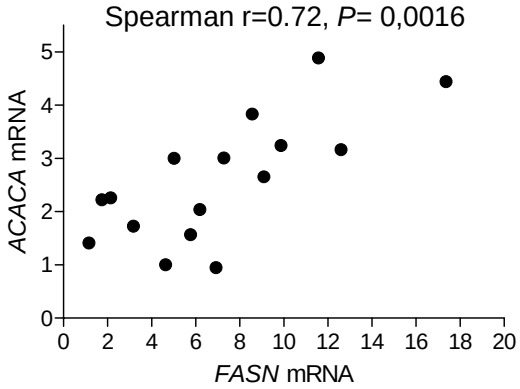

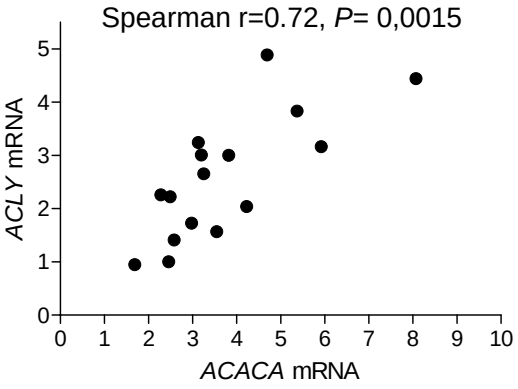

Supplemental Figure 2

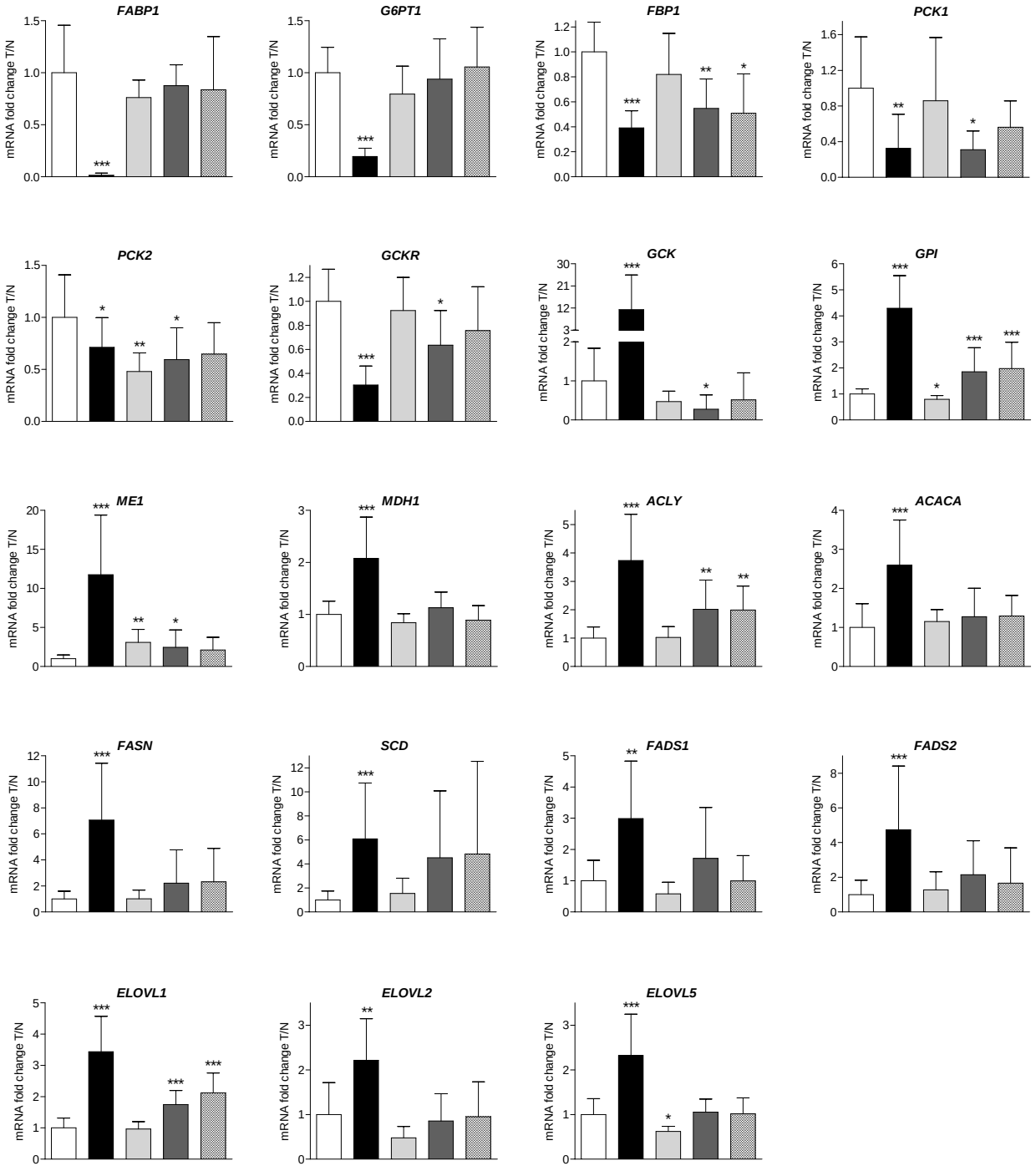

Supplemental Figure 3

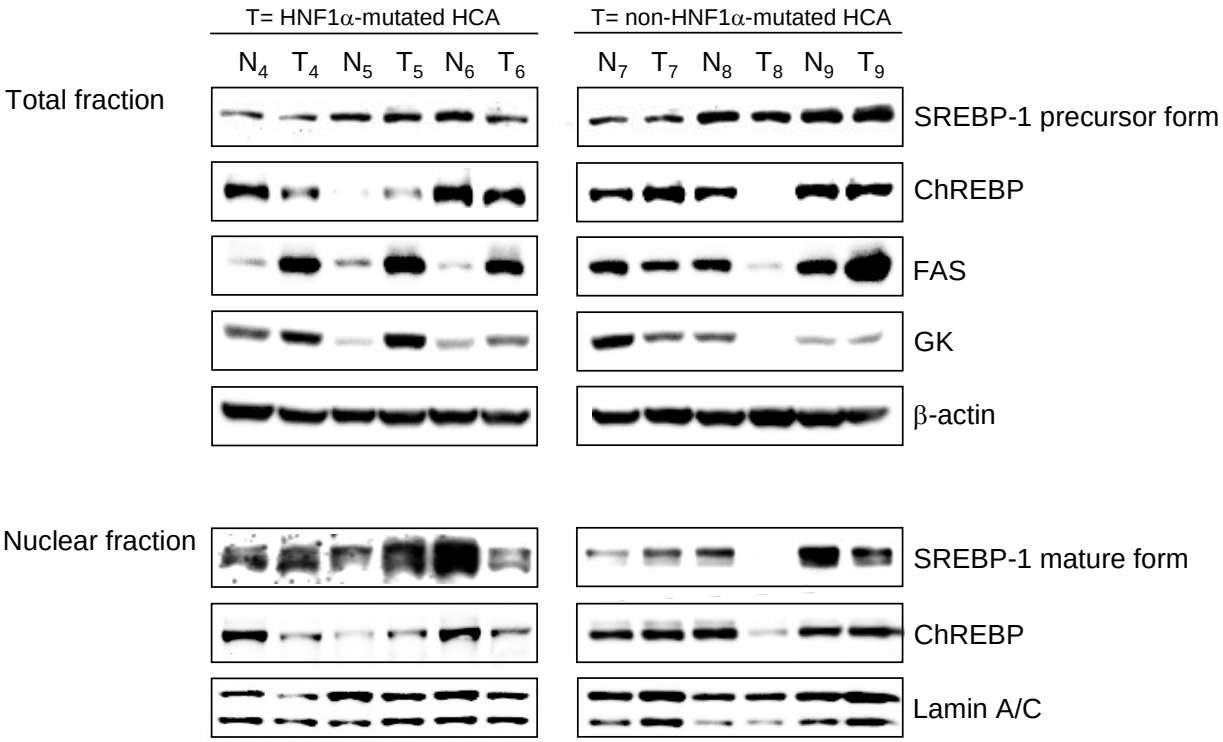

Supplemental Figure 4

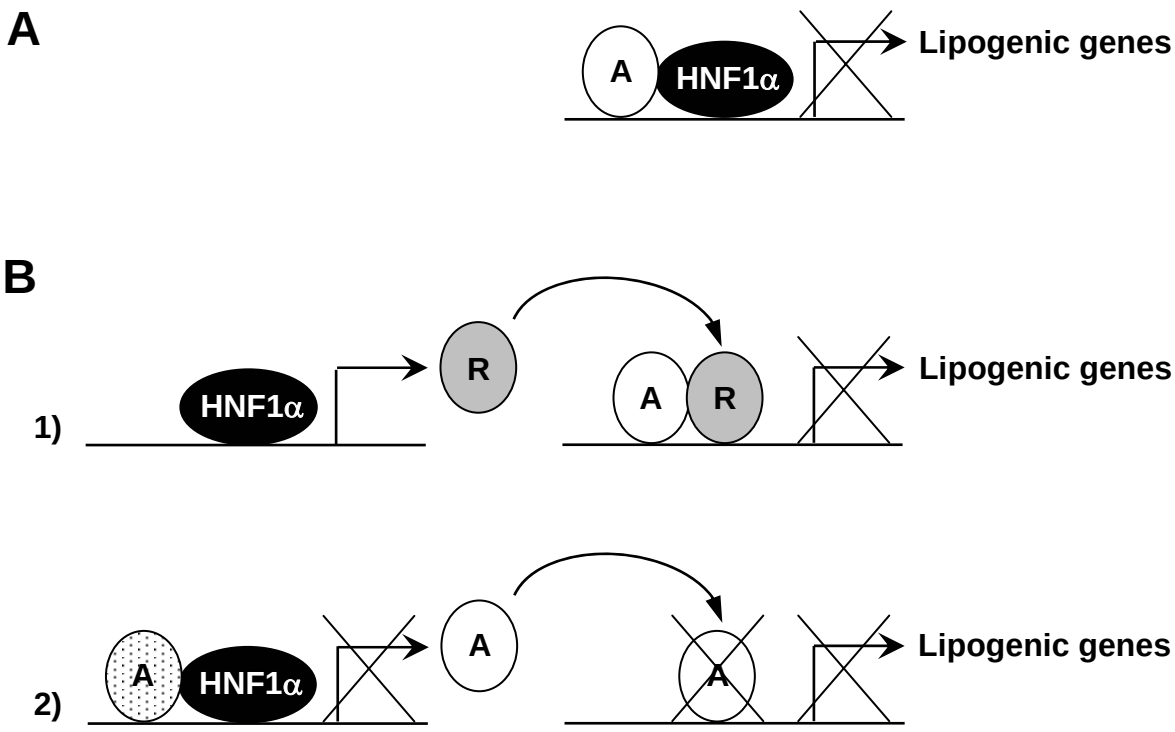

A: transcriptional activator
R: transcriptional repressor